Table 1 Comparisons of clinical and pathological data between "Non-NASH", "borderline NASH" and "NASH" group

	Non-NASH ($n = 4$)	Borderline ($n = 11$)	NASH ($n = 11$)
Age (years)	33.5 ± 12.3	35.1 ± 14.3	46.1 ± 14.8
Sex (female)	2	3	5
BMI (kg/m^2)	28.4 ± 5.1	28.2 ± 5.06	30.4 ± 4.7
AST (U/L)	49.1 ± 62.8	34.1 ± 14.1*	64.2 ± 24.0
ALT (U/L)	65.7 ± 62.6	64.3 ± 40.0	120.5 ± 64.3
GTP (U/L)	42.8 ± 22.1	41.6 ± 14.0	51.5 ± 22.7
Bilirubin (mg/dL)	0.68 ± 0.31	0.68 ± 0.28	0.77 ± 0.38
Albumin (g/dL)	4.41 ± 0.26	4.56 ± 0.33	4.51 ± 0.28
Prothrombin time (%)	97.7 ± 18.1	89.9 ± 12.3	86.7 ± 9.5
Serum ferritin (ng/mL)	199.2 ± 216.5	216.7 ± 195.5	296.2 ± 172.7
Liver histology			
Steatosis (0/1/2/3)	0/4/0/0	0/0/7/4**	0/0/3/8**
Lobular inflammation (0/1/2/3)	0/4/0/0	0/11/0/0	0/5/6/0
Ballooning (0/1/2)	4/0/0$^{\#}$	8/3/0$^{\#\#}$	2/7/2
Stage of fibrosis (0/1/2/3/4)	2/2/0/0/0	2/7/2/0/0	0/7/4/0/0

*$P < 0.05$, $^{\#}P < 0.05$ or $^{\#\#}P < 0.01$vs. NASH; **$P < 0.01$ vs. non-NASH.

Comparisons of clinical and pathological data between "Non-NASH", "borderline NASH" and "NASH" group. NAFLD activity scores were determined according to NASH Clinical Research Network Scoring System.[25] Results are presented as means ± standard deviation for quantitative data, and as numbers for qualitative data. Mann–Whitney U-test for quantitative data or the χ^2 test for qualitative data was performed.

ALT, alanine aminotransferase; AST, aspartate aminotransferase; BMI, body mass index; GTP, γ-glutamyl transpeptidase; NAFLD, non-alcoholic fatty liver disease; NASH, non-alcoholic steatohepatitis; non-NASH, patients with NAFLD activity scores compatible with simple steatosis; Borderline, patients with NAFLD activity scores compatible with borderline NASH; NASH, patients with NAFLD activity scores compatible with NASH.

modalities such as abdominal ultrasonography, computed tomography, and magnetic resonance imaging are anatomical imaging techniques that mainly detect fatty metamorphosis of the liver. No other method has thus far been established for evaluating disease activity and detecting NASH in patients with NAFLD.[28]

Liver/heart ratios as an indicator of intrahepatic ^{99m}Tc-MIBI uptake were significantly lower in patients with NASH compared with those in patients with simple steatosis despite no significant differences in clinical parameters between the groups (Fig. 2 and Table 1). Furthermore, liver/heart ratios were significantly lower in patients with NASH than in healthy volunteers (data not shown). In addition, liver/heart ratios were significantly correlated with NAS (Fig. 3). These data suggest that ^{99m}Tc-MIBI liver scintigraphy would be a useful tool with which to assess NAFLD disease activity and distinguish NASH from simple steatosis.

Liver/heart ratios in patients with no hepatic fibrosis were higher than those in patients with F2 stage of hepatic fibrosis (Fig. 4). However, the degree of hepatic fibrosis was influenced by the degree of NAFLD activity

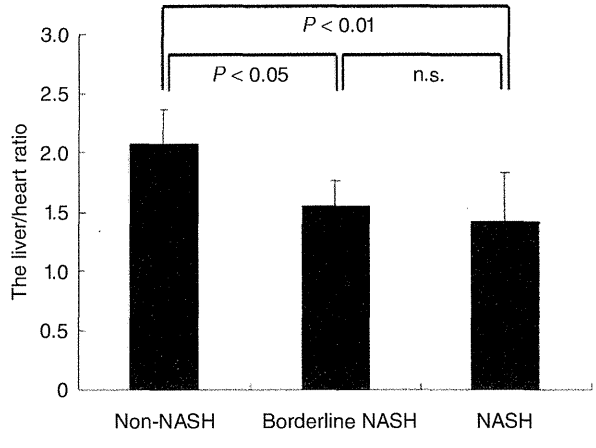

Figure 2 Multiple comparisons of liver/heart ratios on ^{99m}Tc-MIBI scintigraphy among "non-NASH," "borderline NASH," and "NASH" groups. Liver/heart ratios on ^{99m}Tc-MIBI scintigraphy were significantly lower in patients with NASH (1.42 ± 0.41, $P < 0.01$, $n = 11$) and borderline NASH (1.56 ± 0.20, $P < 0.05$, $n = 11$) than in patients with non-NASH (2.07 ± 0.29, $n = 4$) by post-hoc test among three groups. Liver/heart ratio: liver to heart uptake ratio on ^{99m}Tc-MIBI scintigraphy. NASH, non-alcoholic steatohepatitis.

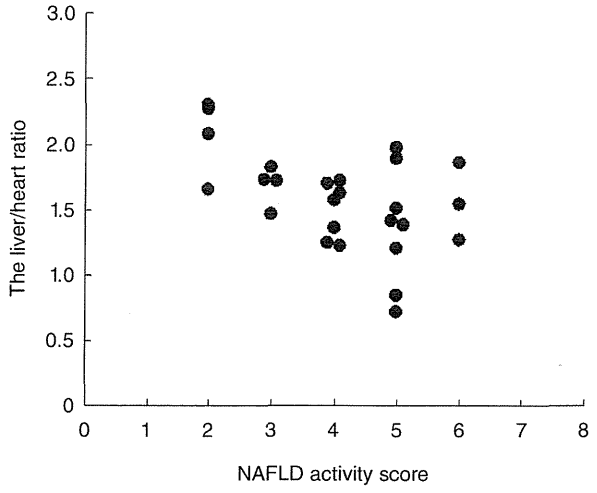

Figure 3 Relationship between non-alcoholic fatty liver disease (NAFLD) activity scores and liver/heart ratio on ^{99m}Tc-MIBI scintigraphy in patients with NAFLD. Liver/heart ratios were significantly correlated with NAFLD activity scores among patients with NAFLD (Spearman's correlation, $r = -0.413$, $P < 0.05$, $n = 26$). Liver/heart ratio: liver to heart uptake ratio on ^{99m}Tc-MIBI scintigraphy.

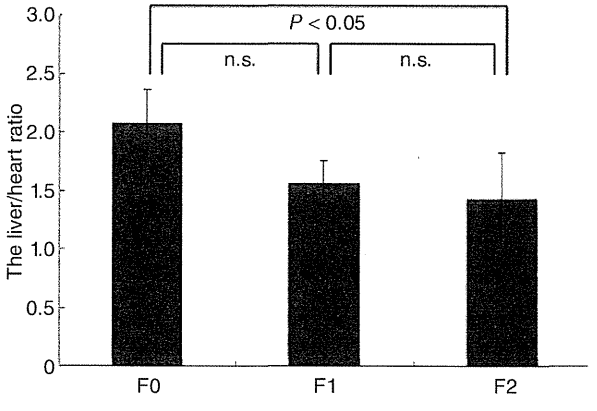

Figure 4 Multiple comparisons of liver/heart uptake ratios on ^{99m}Tc-MIBI scintigraphy based on hepatic fibrosis in patients with non-alcoholic fatty liver disease (NAFLD). Liver/heart ratios on ^{99m}Tc-MIBI scintigraphy were significantly higher in patients with F0 (2.00 ± 0.33, $n = 4$) compared with those in patients with F2 (1.43 ± 0.26, $P < 0.05$, $n = 6$) by post-hoc test among three groups. F0: F0 stage fibrosis. F1: F1 stage fibrosis. F2: F2 stage fibrosis. Hepatic fibrosis was assessed by Brunt's classification (26). Liver/heart ratio: liver to heart uptake ratio on ^{99m}Tc-MIBI scintigraphy.

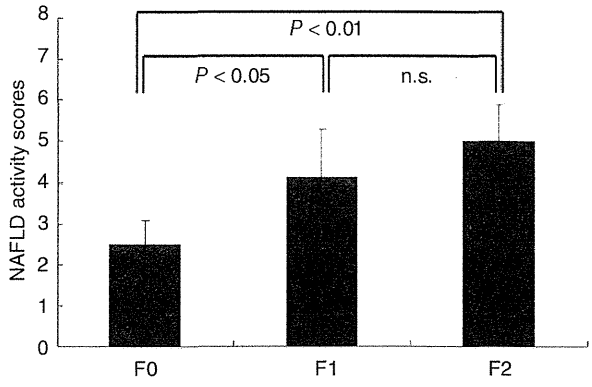

Figure 5 Multiple comparisons of non-alcoholic fatty liver disease (NAFLD) activity scores (NAS) among patients with F0, F1 and F2 stage fibrosis in NAFLD. NAS were significantly lower in patients with F0 (2.5 ± 0.6, $n = 4$) than in patients with F1 (4.1 ± 0.9, $P < 0.05$, $n = 16$) or F2 (5.0 ± 0.9, $P < 0.01$, $n = 6$) by post-hoc test among three groups.

in the present study (Table 1 and Fig. 5). Moreover, no significant correlation was observed between liver/heart ratios and degree of liver fibrosis in this study (data not shown). Taken together, these data suggest that hepatic fibrosis may not be important for liver/heart ratios.

^{99m}Tc-MIBI was originally designed for myocardial perfusion scintigraphy (MPS).[16] The subcellular site of ^{99m}Tc-MIBI retention is the mitochondrion, and its retention is closely related to mitochondrial function.[18,29] In clinical cardiology, with the exception of assessment of myocardial perfusion, ^{99m}Tc-MIBI heart scintigraphy is useful for evaluation of cardiac mitochondrial dysfunction in patients with cardiomyopathy.[19,20] In addition, ^{99m}Tc-MIBI leg scintigraphy is useful for detection of mitochondrial dysfunction in skeletal muscle.[21] Accordingly, in the current study, ^{99m}Tc-MIBI liver scintigraphy by planar imaging was introduced for the first time as a convenient tool for non-invasive assessment of hepatocellular viability based on mitochondrial function in patients with biopsy-proven NAFLD. NASH is now considered, to some extent, to be a mitochondrial disease because mitochondrial dysfunction in the liver would be involved at all successive steps in the induction of NASH.[22] Hepatic mitochondria exhibit ultrastructural lesions, depletion of mitochondrial DNA, and decreased activity of respiratory chain complexes.[22–24] This mitochondrial damage is absent in most patients with simple steatosis and in healthy controls.[24] The present findings suggest that a decrease in intrahepatic ^{99m}Tc-MIBI uptake is connected to NAFLD

disease activity (Fig. 3). A decrease in intrahepatic ^{99m}Tc-MIBI uptake in NAFLD may be a sensitive marker for progression from simple steatosis to NASH.

Cardiovascular disease is a serious prognostic disease for patients with NAFLD. CVD events occur much more frequently in patients with NASH than in those with simple steatosis.[6,30] However, no guidelines for the assessment of myocardial ischemia in NAFLD are currently available. The gold standard for detection of CVD remains invasive angiography with vessel-selective contrast injection of the coronary arteries. This is an invasive procedure with a small but definite risk for complications. Therefore, a non-invasive method for early and accurate diagnosis of both NASH and CVD is needed in the management of NAFLD.

The role of MPS in cardiology has been confirmed to be involved in diagnosis and evaluation of CVD.[15] In particular, exercise or pharmacological stress-inducible hypoperfusion as a marker of ischemia has been validated as a powerful prognostic tool with which to predict adverse cardiovascular outcomes, even in patients with a high likelihood, but unknown presence, of CVD.[31] Stress MPS was recently shown to be essential for screening asymptomatic patients with diabetes at high risk of silent myocardial ischemia.[32] Patients with NAFLD are generally asymptomatic and frequently share several metabolic disorders, including diabetes mellitus type 2, insulin resistance, dyslipidemia, and CVD.[3,5] Moreover, the current body of evidence argues for evaluation of CVD risk in all patients with NAFLD, especially those with NASH.[6] Consequently, it is believed that stress MPS will also play an important role in the identification of a high risk for CVD in patients with NAFLD. Most importantly, MPS must be performed during stress and at rest to detect myocardial ischemia. With the use of a combination of stress and rest tests, ^{99m}Tc-MIBI scintigraphy may have the potential to identify individuals with both CVD and NASH among NAFLD patients. On the other hand, our ^{99m}Tc-MIBI liver scintigraphy by simple planar imaging may be a convenient tool with which to detect NASH among established patients with CVD and NAFLD when cardiologists conduct MPS with ^{99m}Tc-MIBI because performance of identical heart and liver ^{99m}Tc-MIBI scintigraphy series at rest is technically simple. Furthermore, even if patients with NAFLD have normal findings on stress MPS, cardiologists may identify individuals at high risk for CVD by ^{99m}Tc-MIBI liver scintigraphy, because CVD events occur much more frequently in patients with NASH than in patients with simple steatosis.[6,30]

A limitation of this study is that myocardial ^{99m}Tc-MIBI uptake could have influenced the liver/heart ratio if the patients had heart disease such as cardiomyopathy because ROI were set at the liver and heart. Furthermore, a large-scale study is required in the future because the number of patients in this study was small. The future direction of this study is to examine whether ^{99m}Tc-MIBI liver scintigraphy will also be a useful tool for evaluation of the disease activity change in NAFLD after treatment without repeated liver biopsy.

In conclusion, this is the first report to show the usefulness of hepatic ^{99m}Tc-MIBI uptake in evaluation of NAFLD disease activity and discrimination of NASH by focusing on mitochondrial dysfunction in patients with biopsy-proven NAFLD. ^{99m}Tc-MIBI scintigraphy may play an important role in the management of life-threatening comorbidities such as CVD and NASH in patients with NAFLD.

ACKNOWLEDGMENTS

THIS STUDY RECEIVED grants-in-aid for Scientific Research (2010), Grant #20590785, Ministry of Education, Culture, Sports, Science and Technology, Japan.

REFERENCES

1 Angulo P. Nonalcoholic fatty liver disease. *N Engl J Med* 2002; **346**: 1221–31.
2 Ono M, Saibara T. Clinical features of nonalcoholic steatohepatitis in Japan: evidence from the literature. *J Gastroenterol* 2006; **41**: 725–32.
3 Vuppalanchi R, Chalasani N. Nonalcoholic fatty liver disease and nonalcoholic steatohepatitis: selected practical issues in their evaluation and management. *Hepatology* 2009; **49**: 306–17.
4 Bugianesi E, McCullough AJ, Marchesini G. Insulin resistance: a metabolic pathway to chronic liver disease. *Hepatology* 2005; **42**: 987–1000.
5 Grundy SM, Brewer HB Jr, Cleeman JI, Smith SC Jr, Lenfant C. Definition of metabolic syndrome: report of the National Heart, Lung, and Blood Institute/American Heart Association conference on scientific issues related to definition. *Circulation* 2004; **109**: 433–8.
6 Targher G, Day CP, Bonora E. Risk of cardiovascular disease in patients with nonalcoholic fatty liver disease. *N Engl J Med* 2010; **363**: 1341–50.
7 Hamaguchi M, Kojima T, Takeda N *et al.* Nonalcoholic fatty liver disease is a novel predictor of cardiovascular disease. *World J Gastroenterol* 2007; **13**: 1579–84.

8 Targher G, Bertolini L, Poli F *et al.* Nonalcoholic fatty liver disease and risk of future cardiovascular events among type 2 diabetic patients. *Diabetes* 2005; **54**: 3541–6.
9 Targher G, Bertolini L, Rodella S *et al.* Nonalcoholic fatty liver disease is independently associated with an increased incidence of cardiovascular events in type 2 diabetic patients. *Diabetes Care* 2007; **30**: 2119–21.
10 Haring R, Wallaschofski H, Nauck M, Dörr M, Baumeister SE, Völzke H. Ultrasonographic hepatic steatosis increases prediction of mortality risk from elevated serum gamma-glutamyl transpeptidase levels. *Hepatology* 2009; **50**: 1403–11.
11 Targher G, Bertolini L, Padovani R *et al.* Relations between carotid artery wall thickness and liver histology in subjects with nonalcoholic fatty liver disease. *Diabetes Care* 2006; **29**: 1325–30.
12 Adams LA, Lymp JF, St Sauver J *et al.* The natural history of nonalcoholic fatty liver disease: a population-based cohort study. *Gastroenterology* 2005; **129**: 113–21.
13 Rafiq N, Bai C, Fang Y *et al.* Long-term follow-up of patients with nonalcoholic fatty liver. *Clin Gastroenterol Hepatol* 2009; **7**: 234–8.
14 Söderberg C, Stål P, Askling J *et al.* Decreased survival of subjects with elevated liver function tests during a 28-year follow-up. *Hepatology* 2010; **51**: 595–602.
15 Hendel RC, Berman DS, Di Carli MF *et al.* ACCF/ASNC/ACR/AHA/ASE/SCCT/SCMR/SNM 2009 appropriate use criteria for cardiac radionuclide imaging. *Circulation* 2009; **119**: e561–87.
16 Jones AG, Abrams MJ, Davison A *et al.* Biological studies of a new class of technetium complexes: the hexakis(alkylisonitrile)technetium(I) cations. *Int J Nucl Med Biol* 1984; **11**: 225–34.
17 Chiu ML, Kronauge JF, Piwnica-Worms D. Effect of mitochondrial and plasma membrane potentials on accumulation of hexakis (2-methoxyisobutylisonitrile) technetium(I) in cultured mouse fibroblasts. *J Nucl Med* 1990; **31**: 1646–53.
18 Crane P, Laliberté R, Heminway S, Thoolen M, Orlandi C. Effect of mitochondrial viability and metabolism on technetium-99m-sestamibi myocardial retention. *Eur J Nucl Med* 1993; **20**: 20–5.
19 Matsuo S, Nakae I, Tsutamoto T, Okamoto N, Horie M. A novel clinical indicator using Tc-99m sestamibi for evaluating cardiac mitochondrial function in patients with cardiomyopathies. *J Nucl Cardiol* 2007; **14**: 215–20.
20 Unno K, Isobe S, Izawa H *et al.* Relation of functional and morphological changes in mitochondria to myocardial contractile and relaxation reserves in asymptomatic to mildly symptomatic patients with hypertrophic cardiomyopathy. *Eur Heart J* 2009; **30**: 1853–62.
21 Chang YY, Lee CH, Lan MY, Wu HS, Chang CC, Liu JS. A new noninvasive test to detect mitochondrial dysfunction of skeletal muscles in progressive supranuclear palsy. *Ann N Y Acad Sci* 2005; **1042**: 76–81.
22 Pessayre D, Fromenty B. NASH: a mitochondrial disease. *J Hepatol* 2005; **42**: 928–40.
23 Caldwell SH, Swerdlow RH, Khan EM *et al.* Mitochondrial abnormalities in non-alcoholic steatohepatitis. *J Hepatol* 1999; **31**: 430–4.
24 Sanyal AJ, Campbell-Sargent C, Mirshahi F *et al.* Nonalcoholic steatohepatitis: association of insulin resistance and mitochondrial abnormalities. *Gastroenterology* 2001; **120**: 1183–92.
25 Kleiner DE, Brunt EM, Van Natta M *et al.* Design and validation of a histological scoring system for nonalcoholic fatty liver disease. *Hepatology* 2005; **41**: 1313–21.
26 Brunt EM, Janney CG, Di Bisceglie AM, Neuschwander-Tetri BA, Bacon BR. Nonalcoholic steatohepatitis: a proposal for grading and staging the histological lesions. *Am J Gastroenterol* 1999; **94**: 2467–74.
27 Merriman RB, Ferrell LD, Patti MG *et al.* Correlation of paired liver biopsies in morbidly obese patients with suspected nonalcoholic fatty liver disease. *Hepatology* 2006; **44**: 874–80.
28 Wieckowska A, McCullough AJ, Feldstein AE. Noninvasive diagnosis and monitoring of nonalcoholic steatohepatitis: present and future. *Hepatology* 2007; **46**: 582–9.
29 Arbab AS, Koizumi K, Toyama K, Arai T, Araki T. Technetium-99m-tetrofosmin, technetium-99m-MIBI and thallium-201 uptake in rat myocardial cells. *J Nucl Med* 1998; **39**: 266–71.
30 Ekstedt M, Franzen LE, Mathiesen UL *et al.* Long-term follow-up of patients with NAFLD and elevated liver enzymes. *Hepatology* 2006; **44**: 865–73.
31 Hachamovitch R, Hayes SW, Friedman JD, Cohen I, Berman DS. Stress myocardial perfusion single-photon emission computed tomography is clinically effective and cost effective in risk stratification of patients with a high likelihood of coronary artery disease (CAD) but no known CAD. *J Am Coll Cardiol* 2004; **43**: 200–8.
32 Yamasaki Y, Nakajima K, Kusuoka H *et al.* Prognostic value of gated myocardial perfusion imaging for asymptomatic patients with type 2 diabetes: the J-ACCESS 2 investigation. *Diabetes Care* 2010; **33**: 2320–6.

2 Redaelli CA, Tian YH, Schaffner T, Ledermann M, Baer HU, Dufour JF. Extended preservation of rat liver graft by induction of heme oxygenase-1. *Hepatology* 2002; **35**: 1082–92.
3 Wang C, Wang Z, Tao S *et al.* Preconditioning donor liver with *Nodosin* perfusion lessens rat ischemia reperfusion injury via heme oxygenase-1 upregulation. *J. Gastroenterol. Hepatol.* 2012; **27**: 832–40.
4 Yachie A, Niida Y, Wada T *et al.* Oxidative stress causes enhanced endothelial cell injury in human heme oxygenase-1 deficiency. *J. Clin. Invest.* 1999; **103**: 129–35.
5 Poss KD, Tonegawa S. Heme oxygenase 1 is required for mammalian iron reutilization. *Proc. Natl. Acad. Sci. U.S.A.* 1997; **94**: 10919–24.
6 Soares MP, Brouard S, Smith RN, Bach FH. Heme oxygenase-1, a protective gene that prevents the rejection of transplanted organs. *Immunol. Rev.* 2001; **184**: 275–85.
7 DeBruyne LA, Magee JC, Buelow R, Bromberg JS. Gene transfer of immunomodulatory peptides correlates with heme oxygenase-1 induction and enhanced allograft survival. *Transplantation* 2000; **69**: 120–8.
8 Otterbein LE, Mantell LL, Choi AM. Carbon monoxide provides protection against hyperoxic lung injury. *Am. J. Physiol.* 1999; **276**: L688–94.
9 Sato K, Balla J, Otterbein L *et al.* Carbon monoxide generated by heme oxygenase-1 suppresses the rejection of mouse-to-rat cardiac transplants. *J. Immunol.* 2001; **166**: 4185–94.
10 Baranano DE, Rao M, Ferris CD, Snyder SH. Biliverdin reductase: a major physiologic cytoprotectant. *Proc. Natl. Acad. Sci. U.S.A.* 2002; **99**: 16093–8.
11 Yamashita K, McDaid J, Ollinger R *et al.* Biliverdin, a natural product of heme catabolism, induces tolerance to cardiac allografts. *FASEB J.* 2004; **18**: 765–7.
12 Wang H, Lee SS, Dell'Agnello C *et al.* Bilirubin can induce tolerance to islet allografts. *Endocrinology* 2006; **147**: 762–8.
13 Ferris CD, Jaffrey SR, Sawa A *et al.* Haem oxygenase-1 prevents cell death by regulating cellular iron. *Nat. Cell Biol.* 1999; **1**: 152–7.
14 Berberat PO, Katori M, Kaczmarek E *et al.* Heavy chain ferritin acts as an antiapoptotic gene that protects livers from ischemia reperfusion injury. *FASEB J.* 2003; **17**: 1724–6.
15 Shen B, Yu J, Wang S *et al.* Phyllanthus urinaria ameliorates the severity of nutritional steatohepatitis both *in vitro* and *in vivo*. *Hepatology* 2008; **47**: 473–83.

Is impaired Kupffer cell function really important to the pathogenesis of nonalcoholic steatohepatitis?

Masafumi Ono and Toshiji Saibara

Department of Gastroenterology and Hepatology, Kochi Medical School, Kochi, Japan

See article in *J. Gastroenterol. Hepatol.* 2012; 27: 789–796.

Accepted for publication 1 January 2012.

Correspondence
Dr Masafumi Ono, Department of Gastroenterology and Hepatology, Kochi Medical School, Kohasu, Oko-cho, Nankoku, Kochi 783-8505, Japan. Email: onom@kochi-u.ac.jp

Nonalcoholic fatty liver disease (NAFLD) is now the most common cause of chronic liver disease worldwide. Nonalcoholic steatohepatitis (NASH) is a progressive form of NAFLD with the potential for progression to cirrhosis. The pathogenesis of NASH is incompletely understood, but may involve hyperendotoxemia[1] secondary to impaired phagocytotic function of Kupffer cells (KCs)[2] and consequent KC overproduction of and increased sensitivity to cytokines such as tumor necrosis factor (TNF)-α and interleukin-1β (IL-1β).[3] Impaired phagocytotic function of KCs may therefore lead to higher endotoxin levels in the systemic circulation, as has been observed in patients with NASH and in animal models of NASH.[4]

Kupffer cells are liver-resident macrophages that provide important protection against the emergence of endotoxins and harmful exogenous particles from the portal vein to the systemic circulation.[5] KCs differ in their morphological characteristics, physiological functions, and population density in the liver acinus. Those localized in the periportal zone express the scavenger receptor CD163, also described as ED2 antigen, and exhibit higher activity of phagocytosis and lysosomal protease activity as well as greater release more biological active mediators, such as cytokines, than KCs located in the perivenous and midzonal areas.[6] By contrast, glycosylated transmembrane protein CD68 (ED1) is detected in all KCs regardless of acinar location. Increased expression of CD68-positive KCs is related to the histological severity of the livers of patients with NAFLD. In addition, aggregates of enlarged KCs exist in perivenular regions of the livers of patients with NASH compared with the diffuse distribution seen in simple steatosis (SS).[7]

Absent KCs or impaired KC function may be associated with harmful effects. Resultant impaired clearance of bacterial products, lipopolysaccharides (LPS), endotoxins, and other dangerous molecules may accelerate pathogenesis of liver diseases. Depletion of KCs by gadolinium chloride ($GdCl_3$) or clodronate liposomes has been reported to shift the distribution of phagocytosis and alter the balance of cytokines release, thereby reflecting the functional complexity and phenotypic plasticity of KCs.[8] In contrast, when ED2-positive KCs are selectively depleted by $GdCl_3$ or clodronate, liver diseases induced by alcohol, carbon tetrachloride, thioacetamide, and ischemia/reperfusion are remarkably attenuated. In addition, deletion of ED2-positive KCs by $GdCl_3$ or clodronate attenuates proinflammatory and profibrogenic cytokine release, thereby protecting fatty livers from progression to NASH. In summary, these results indicate that ED2-positive KCs are involved in the progression of various kinds of liver disease, including NASH.

Most LPS in the body is produced in the gastrointestinal (GI) tract and enters the liver through the portal vein. The liver is the final barrier to prevent GI bacteria and LPS from entering the systemic circulation. Because of the location of KCs in the liver sinusoids, which drain the GI tract through the portal vein, KCs are chronically exposed to higher concentrations of LPS than are peripheral macrophages. Therefore, impaired phagocytotic function of KCs leads to elevation of circulating LPS in experimental models of NASH.[9] Elevation of circulating LPS from the GI tract is also considered important in the pathogenesis for NASH because control of bacterial overgrowth in the GI tract by administration of probiotics led to improvement of NASH.[10,11]

Given that overproduction and increased sensitivity to cytokines such as TNF-α and IL-1β from KCs[3,4] is also implicated in the

pathogenesis of NASH, failure of KCs to clear endotoxins and LPS because of defective phagocytotic function may further drive the production of these proinflammatory cytokines by KCs. On the other hand, it is also considered that KCs that produce cytokines may differ from KCs with phagocytotic activity, and LPS-responsive KCs (CD14-positive KCs) are potential sources of proinflammatory and profibrogenic cytokine release. Cytokines such IL-1, IL-6, and TNF-α are released from CD14-positive KCs by stimulation of LPS.[12] CD14-transgenic mice that overexpress CD14 on monocytes have increased sensitivity to LPS.[13] In contrast, CD14-deficient mice are completely unable to release cytokine when exposed to LPS.[14] Even when the CD14 expression on KCs is low, CD14 is still critical for LPS activation. In addition, isolated KCs respond to low concentrations of LPS with production of proinflammatory cytokines. Although the expression of CD14-positive KCs is low in normal livers,[15] these cells increase in many types of liver disease by progression of hepatic fibrosis, advanced stage, and stimulation of LPS.[16]

Superparamagnetic iron oxide (SPIO) magnetic resonance imaging (SPIO-MRI) is a popular liver-specific MRI method for detecting hepatocellular carcinomas (HCCs).[17] The technique relies on the ability of KCs to take up SPIO particles. Because KCs are absent in HCC tissues, differential phagocytosis of SPIO particles allows radiological separation of normal liver from HCC lesions. Following intravenous SPIO, phagocytosis by KCs leads to reduced signal intensity on T2 MRI sequences such that HCCs with no KCs show high signal intensity. Conversely, areas with abundant KCs show low T2 signal intensity. In normal liver, therefore, there is a low T2 signal intensity. The signal intensity using SPIO can serve as a surrogate marker of KC phagocytotic function. SPIO-MRI, therefore, was also established and introduced to evaluate phagocytotic function of KCs in humans and rats with NAFLD.[18,19] An ultrasonographic technique was also introduced to evaluate the phagocytotic function of KCs in patients with NASH.[20] Furthermore, phagocytosis of KCs was impaired in patients with NASH, and the methods were useful for evaluating the phagocytotic function of KCs. However, ultrasonographic evaluation of phagocytotic function of KCs may be influenced by altered hepatic microcirculation. On the other hand, SPIO-MRI methods control for possible microcirculatory changes.[19] Therefore, as in this study, SPIO-MRI is a useful method for evaluating phagocytotic function of KCs in patients with NAFLD.

In this issue of the *Journal of Gastroenterology and Hepatology*,[21] Tonan *et al.* clearly showed that the number of CD14-positive KCs in the livers of patients with NASH increased compared with that in patients with SS, although the number of CD-68-positive KCs was not different. This result may indicate that the sensitivity for LPS and endotoxin might increase in the livers of patients with NASH compared with SS, and hypersensitivity for LPS may be an important pathogenic factor for progression of NASH. Activation of CD14-positive KCs and elevation of the LPS concentration promote the activation of proinflammatory cytokine release, which leads to the development of NASH. Therefore, as they showed, the number of CD14-positive KCs might be correlated to the degree of necroinflammation and severity of fibrosis in the livers of patients with NASH. CD14-positive KCs were reportedly physiologically associated with septal myofibroblasts expressing α-smooth muscle actin. This finding raises the possibility that LPS and CD14-positive KCs may be involved in fibrosis across a broad spectrum of liver diseases. In addition, impaired phagocytotic function of KCs evaluated by SPIO-MRI methods was not correlated to the total number of KCs, but to the number of CD14-positive KCs in this study.

As already noted, impaired phagocytotic function of KCs may cause elevation of the circulating LPS concentration. They also showed that the degree of impaired phagocytotic function of KCs was correlated to the degree of necroinflammation and severity of fibrosis in the livers of patients with NASH, although it was previously reported that severity of NASH, grading, and staging were not related to the impairment of KC phagocytotic function.[19] The mechanism underlying the observed impaired phagocytotic function of KCs also remains unclear. However, impaired phagocytotic function of KCs may influence the increased expression of CD14-positive KCs and sensitivity for LPS and lead to hyper-release of proinflammatory cytokines and progression of NASH. These results indicate that impaired phagocytotic function of KCs may also be an important pathogenic factor for progression of NASH. In conclusion, the question remains: is impaired Kupffer cell function really important to the pathogenesis of NASH? We believe that impaired Kupffer cell function is really important to the pathogenesis of NASH, a contention that receives further support by these elegant imaging studies by Tonan and colleagues. Further mechanistic studies are indicated to clarify the pathogenic mechanisms of KC function impairment in NASH.

References

1 Creely SJ, McTernan PG, Kusminski CM *et al.* Lipopolysaccharide activates an innate immune system response in human adipose tissue in obesity and type 2 diabetes. *Am. J. Physiol. Endocrinol. Metab.* 2007; **292**: E740–7.
2 Loffreda S, Yang SQ, Lin HZ *et al.* Leptin regulates proinflammatory immune responses. *FASEB J.* 1998; **12**: 57–65.
3 Diehl AM. Nonalcoholic steatosis and steatohepatitis IV. Nonalcoholic fatty liver disease abnormalities in macrophage function and cytokines. *Am. J. Physiol. Gastrointest. Liver Physiol.* 2002; **282**: G1–5.
4 Solga SF, Diehl AM. Non-alcoholic fatty liver disease: lumen-liver interactions and possible role for probiotics. *J. Hepatol.* 2003; **38**: 681–7.
5 Fox ES, Broitman SA, Thomas P. Bacterial endotoxins and the liver. *Lab. Invest.*1990; **63**: 733–41.
6 Laskin DL, Weinberger B, Laskin JD. Functional heterogeneity in liver and lung macrophages. *J. Leukoc. Biol.* 2001; **70**: 163–70.
7 Park JW, Jeong G, Kim SJ, Kim MK, Park SM. Predictors reflecting the pathological severity of non-alcoholic fatty liver disease: comprehensive study of clinical and immunohistochemical findings in younger Asian patients. *J. Gastroenterol. Hepatol.* 2007; **22**: 491–7.
8 Baffy G. Kupffer cells in non-alcoholic fatty liver disease: the emerging view. *J. Hepatol.* 2009; **51**: 212–23.
9 Yang SQ, Lin HZ, Lane MD, Clemens M, Diehl AM. Obesity increases sensitivity to endotoxin liver injury: implications for the pathogenesis of steatohepatitis. *Proc. Natl. Acad. Sci. U.S.A.* 1997; **94**: 2557–62.
10 Velayudham A, Dolganiuc A, Ellis M *et al.* VSL#3 probiotic treatment attenuates fibrosis without changes in steatohepatitis in a diet-induced nonalcoholic steatohepatitis model in mice. *Hepatology* 2009; **49**: 989–97.
11 Li Z, Yang S, Lin H *et al.* Probiotics and antibodies to TNF inhibit inflammatory activity and improve nonalcoholic fatty liver disease. *Hepatology* 2003; **37**: 343–50.

12 Su GL. Lipopolysaccharides in liver injury: molecular mechanisms of Kupffer cell activation. *Am. J. Physiol.* 2002; **283**: G256–65.
13 Ferrero E, Jiao D, Tsuberi BZ *et al.* Transgenic mice expressing human CD14 are hypersensitive to lipopolysaccharide. *Proc. Natl. Acad. Sci. U.S.A.* 1993; **90**: 2380–4.
14 Haziot A, Ferrero E, Köntgen F *et al.* Resistance to endotoxin shock and reduced dissemination of gram-negative bacteria in CD14-deficient mice. *Immunity* 1996; **4**: 407–14.
15 Ikejima K, Enomoto N, Seabra V, Ikejima A, Brenner DA, Thurman RG. Pronase destroys the lipopolysaccharide receptor CD14 on Kupffer cells. *Am. J. Physiol.* 1999; **276**: G591–8.
16 Leicester KL, Olynyk JK, Brunt EM, Britton RS, Bacon BR. Differential findings for CD14-positive hepatic monocytes/macrophages in primary biliary cirrhosis, chronic hepatitis C and nonalcoholic steatohepatitis. *Liver Int.* 2006; **26**: 559–65.
17 Ward J, Guthrie JA, Scott DJ *et al.* Hepatocellular carcinoma in the cirrhotic liver: double-contrast MR imaging for diagnosis. *Radiology* 2000; **216**: 154–62.
18 Tomita K, Tanimoto A, Irie R *et al.* Evaluating the severity of nonalcoholic steatohepatitis with superparamagnetic iron oxide-enhanced magnetic resonance imaging. *J. Magn. Reson. Imaging* 2008; **28**: 1444–50.
19 Asanuma T, Ono M, Kubota K *et al.* Super paramagnetic iron oxide MRI shows defective Kupffer cell uptake function in non-alcoholic fatty liver disease. *Gut* 2010; **59**: 258–66.
20 Moriyasu F, Iijima H, Tsuchiya K *et al.* Diagnosis of NASH using delayed parenchymal imaging of contrast ultrasound. *Hepatol. Res.* 2005; **33**: 97–9.
21 Tonan T, Fujimoto K, Qayyum A *et al.* CD14 expression and Kupffer cell dysfunction in non-alcoholic steatohepatitis: Superparamagnetic iron oxide-magnetic resonance image and pathologic correlation. *J. Gastroenterol. Hepatol.* 2012; **27**: 789–96.

Asian consensus report on functional dyspepsia: Necessary and ready?

Justin C Y Wu

Institute of Digestive Disease, The Chinese University of Hong Kong, Hong Kong SAR

See article in *J. Gastroenterol. Hepatol.* 2012; 27: 626–641.

Functional dyspepsia is one of the commonest digestive disorders, which affects 10–20% of the adult population worldwide. Although it is not associated with excessive mortality, patients with functional dyspepsia often suffer from significant morbidity with functional impairment, loss of working days, and workload burden on the healthcare system.

Despite the high prevalence and major impact in the community, the importance of functional dyspepsia has been relatively ignored in Asia. In the past two decades, there have been major breakthroughs in the diagnosis and treatment of *Helicobacter pylori* infection, peptic ulcer, gastric cancer and non-variceal upper gastrointestinal bleeding. On the other hand, there remain a lot of mysteries for functional dyspepsia. The etiology and mechanism of functional dyspepsia are heterogeneous and poorly understood. None of the reported pathophysiologic features are consistently observed in all patients and therefore there is no diagnostic biomarker. As a result, the diagnosis and classification of functional dyspepsia are empirical and primarily symptom-based. Furthermore, the diagnostic criteria and classification scheme have been changing in the past two decades. Management of functional dyspepsia has been disappointing and effective treatment is still lacking.

In this issue of JGH, a consensus report on functional dyspepsia has been prepared by a group of opinion leaders in Asia.[1] In this report, a critical appraisal is conducted on various topics related to functional dyspepsia in Asia. There is also a comprehensive review on the current practice, which includes diagnosis and management, of functional dyspepsia.

There are several merits in this report. The report highlights some distinct clinical characteristics of functional dyspepsia that are unique to Asian patients. For example, Asian patients tend to have higher proportion of postprandial distress syndrome. Some important differential diagnoses of dyspepsia, which are far less common in Western population, are emphasized. These include parasitic infestation and hepatocellular carcinoma due to high prevalence of chronic hepatitis B infection in this region. Instead of endorsing the statements of the Rome criteria, this report casts doubt on the validity of the Rome diagnostic criteria for functional dyspepsia in Asian patients. Since dyspepsia is transient and self-limiting in many patients, it is prudent for the Rome criteria to establish a minimum requirement of 6 months for the diagnosis so as to avoid over-diagnosis.[2] However, significant morbidity occurs as early as 4 weeks after the onset of dyspepsia in many Asian patients. Furthermore, owing to the marked ethnic difference in cultural and linguistic origin, there may be substantial variation in the accuracy of Rome criteria in Asian population and further validation studies are needed. For the management of functional dyspepsia, this report also underscores the possible inferior therapeutic benefit of proton pump inhibitor, presumably due to the lower prevalence of gastroesophageal reflux disease in Asian patients with functional dyspepsia.

Helicobacter pylori infection is another important topic that is significantly different from the Western counterparts. In the Rome criteria, there is no need to exclude *H. pylori* infection for the diagnosis of functional dyspepsia. Compared with the Western population, however, the prevalence of *H. pylori* and its related diseases such as peptic ulcer and gastric cancer are much higher in Asian population. These conditions are the major differential diagnoses of functional dyspepsia, even in the absence of alarm symptom. Furthermore, the prevalence of a virulent strain of *H. pylori* is substantially higher in Asian populations. It has also been postulated that severe corpus-predominant gastritis is more commonly seen in Asian patients.[3] This may contribute to higher risk of gastric atrophy and gastric cancer. Owing to these virulent factors, it has been proposed that *H. pylori* may be directly related to dyspepsia in Asian patients and therefore *H. pylori* infection should be excluded to make a diagnosis of functional dyspepsia.

Accepted for publication 25 January 2012.

Correspondence
Justin C Y Wu, Department of Medicine and Therapeutics, 9/F, Prince of Wales Hospital, Shatin, Hong Kong. Email: justinwu@cuhk.edu.hk

OPEN ACCESS Freely available online

PLoS one

BART Inhibits Pancreatic Cancer Cell Invasion by PKCα Inactivation through Binding to ANX7

Keisuke Taniuchi[1]*, Kunihiko Yokotani[1], Toshiji Saibara[2]

1 Department of Pharmacology, School of Medicine, Kochi University, Nankoku, Kochi, Japan, **2** Department of Gastroenterology and Hepatology, School of Medicine, Kochi University, Nankoku, Kochi, Japan

Abstract

A novel function for the binder of Arl two (BART) molecule in pancreatic cancer cells is reported. BART inhibits invasiveness of pancreatic cancer cells through binding to a Ca^{2+}-dependent, phosphorylated, guanosine triphosphatase (GTPase) membrane fusion protein, annexin7 (ANX7). A tumor suppressor function for ANX7 was previously reported based on its prognostic role in human cancers and the cancer-prone mouse phenotype *ANX7*(+/−). Further investigation demonstrated that the BART–ANX7 complex is transported toward cell protrusions in migrating cells when BART supports the binding of ANX7 to the protein kinase C (PKC) isoform PKCα. Recent evidence has suggested that phosphorylation of ANX7 by PKC significantly potentiates ANX7-induced fusion of phospholipid vesicles; however, the current data suggest that the BART–ANX7 complex reduces PKCα activity. Knocking down endogenous BART and ANX7 increases activity of PKCα, and specific inhibitors of PKCα significantly abrogate invasiveness induced by BART and ANX7 knockdown. These results imply that BART contributes to regulating PKCα activity through binding to ANX7, thereby affecting the invasiveness of pancreatic cancer cells. Thus, it is possible that BART and ANX7 can distinctly regulate the downstream signaling of PKCα that is potentially relevant to cell invasion by acting as anti-invasive molecules.

Citation: Taniuchi K, Yokotani K, Saibara T (2012) BART Inhibits Pancreatic Cancer Cell Invasion by PKCα Inactivation through Binding to ANX7. PLoS ONE 7(4): e35674. doi:10.1371/journal.pone.0035674

Editor: Fazlul H. Sarkar, Wayne State University School of Medicine, United States of America

Received January 29, 2012; **Accepted** March 19, 2012; **Published** April 19, 2012

Funding: This work was supported by a Grant-in-Aid from the Ministry of Health, Labour, and Welfare of Japan. The funders had no role in study design, data collection and analysis, decision to publish, or preparation of the manuscript.

Competing Interests: The authors have declared that no competing interests exist.

* E-mail: ktaniuchi@kochi-u.ac.jp

Introduction

The binder of Arl two (BART) molecule is a soluble 19-kDa protein originally purified from bovine brain and identified as a binding partner of ADP-ribosylation factor-like 2 (ARL2) [1]. The binding of BART to ARL2 is of high affinity and dependent on the binding of GTP to ARL2 [1]. Distinct functions have been inferred from findings that ARLs lack the biochemical or genetic activities characteristic of ADP ribosylation factors (ARFs), despite the 40% to 60% amino acid sequence identity between ARFs and ARLs [2]. ARL2 has been implicated as a regulator of microtubule dynamics and folding [3], but its function remains largely unknown. We previously reported that regulation of BART post-transcriptional modification *via* intracellular CD24 binding to G3BP in stress granules contributes to inhibition of invasion and metastasis of pancreatic ductal adenocarcinoma (PDAC) cells [4]. N-terminal G3BP contributes to post-transcriptional regulation of BART [5]. Further study demonstrated that BART decreases invasiveness of PDAC cells by inhibiting the ARL2-mediated decrease in the activity of the Rho GTPase protein RhoA [6]. These data suggest that BART plays a role in inhibition of PDAC invasiveness.

ANX7 is a member of the annexin family of calcium-dependent phospholipid binding proteins and codes for a Ca^{2+}-activated GTPase. *ANX7*(+/−) knockout mice have Ca^{2+}-dependent endocrine secretory defects [7]. ANX7 is phosphorylated by PKC, which significantly enhances binding of ANX7 to fused phospholipid vesicles in chromaffin cells [8]. Activated PKCs induce the secretion of MMP-9, lead to activation of MMP-2, downregulate TIMP-1 and TIMP-2 secretion, and increase MT1-MMP on the cell surface [9]. Thus, ANX7 may be one of the factors associated with the PKC-dependent secretion cascade. Furthermore, ANX7 is a newly described tumor suppressor gene for prostate cancer, as evidenced by loss of heterozygosity and reduced ANX7 protein expression in a large fraction of archived metastatic tumors [10]. ANX7 exhibits many biological and genetic properties of a tumor suppressor gene and is also implicated in carcinogenesis through discrete signaling pathways involving other tumor suppressors, DNA-repair and apoptosis-related genes [10,11]. These reports have suggested that ANX7 plays several different roles involved in exocytosis, tumor suppression and carcinogenesis.

PKC is a family of serine/threonine kinases involved in the transduction of signals, including the Ras signal, for cell proliferation and differentiation [12,13]. The PKC family consists of at least 12 isoforms with different tissue expression patterns, substrate specificities, and subcellular localizations that are related to specialized cell functions, including cell proliferation, differentiation, and apoptosis [14]. The 'classical' PKCs (α, β1, β2, and γ) bind phorbol esters and are Ca^{2+} dependent. The 'novel' PKCs (δ, ε, η, and θ) do not depend on Ca^{2+}, but do bind phorbol esters. The third subfamily comprises the 'atypical' PKCs (ξ, ι, λ, and μ), which do not bind to either Ca^{2+} or phorbol ester [14,15]. Constitutively activated cell surface receptors, such as the EGF receptor or the PDGF receptor [16], or Ras [17], cause

hyperactivation of PKC as well as the mitogen-activated protein kinase (MAPK) cascade. Overexpression of PKCδ induces a more malignant pancreatic cancer cell phenotype *in vivo*, through modulation of cell proliferation and survival [18]. Another study demonstrated that activated PKC induces lamellipodia formation and subsequent increased migratory activity of subconjunctival fibroblasts [19]. Thus, it has been suggested that PKCs induce cell proliferation/survival, invasion and metastasis.

In this study, ANX7 was identified as a novel binding partner of BART, and BART was found to be associated with ANX7-PKC complex formation in PDAC cells. Furthermore, the current results demonstrated that knocking down BART induces cell invasion by increasing PKCα activity through the loss of ANX7-PKCα complex formation. Thus, decreased active PKCα *via* both BART and ANX7 contributes to inhibition of PDAC invasiveness.

Results

BART binds to ANX7 in PDAC cells

BART knockdown increases retroperitoneal invasion and PDAC cell metastasis to liver in an orthotopic xenograft model, as described in a previous report [4]. To investigate the mechanism by which BART suppresses invasiveness and metastasis, immunoprecipitation (IP) experiments were performed in the human PDAC cell line S2-013 using a specific antibody to BART, to detect complexes of BART with other proteins. S2-013 is a cloned subline of a PDAC cell line (SUIT-2) derived from a liver metastasis [20], and was obtained from Dr. T. Iwamura (Miyazaki Medical College, Miyazaki, Japan). Silver-stained immunoprecipitated fractions separated on SDS-PAGE gels revealed a 50-kDa band that was not seen in the isotype control immunoprecipitates (arrow in Fig. 1A). The band was excised and analyzed by Q-TOF-MS after in-gel trypsin digestion, and identified as ANX7. The peptide sequence coverage was 15% (Fig. 1B). This specific binding of ANX7 to BART was demonstrated by co-IP from S2-013 cells (Fig. 1C) and subcellular colocalization was analyzed by immunostaining of S2-013 cells (Fig. 1D). BART and ANX7 coimmunoprecipitated and were colocalized in the cytoplasm. Of note is that BART and ANX7 accumulated in lamellipodial-like protrusions that are essential for cell migration (arrows in Fig. 1E).

ANX7 inhibits PDAC cell invasion

Previously, cell clones were generated in which BART was stably suppressed by vector-based specific short hairpin small interfering RNA (siRNA) in S2-013 cells that formerly expressed high levels of BART [4]. To determine the function of BART-ANX7 complexes, a wound-healing immunostaining assay was used to observe the localization of BART and ANX7 in polarized migrating cells (Fig. 2A). Both BART and ANX7 were recruited to the leading edges during wound healing of control S2-013 cells (arrows in Fig. 2A). Depletion of BART inhibited ANX7 accumulation at the leading edges (lower panels in Fig. 2A). Combined with the result of Fig. 1E, these results indicate that BART and ANX7 interdependently localize at the leading edges and in the lamellipodial-like protrusions associated with cell migration.

In vitro assays were used to examine the effects of ANX7 on cell motility and invasion. As shown by Western blot analysis, ANX7 expression was markedly reduced in S2-013 and a PDAC cell line, PANC-1, 72 h after transfection with the ANX7-targeting siRNA oligonucleotides, in contrast to cells transfected with scrambled siRNA-oligonucleotides (Fig. 2B). Suppression of ANX7 enhanced motility in transwell motility assays of S2-013 and PANC-1 as compared to control cells (Fig. 2C). In two-chamber invasion assays, ANX7 RNAi cells were significantly more invasive than the control S2-013 and PANC-1 cells (Fig. 2D). These results suggest an important role for the binding of BART and ANX7 in inhibition of cell migration.

Binding of ANX7 and phosphorylated PKC is associated with inhibiting invasiveness of PDAC cells

Co-IP of the ANX7 and PKC complex was performed using anti-ANX7 or anti-PKC antibody (10800) reacting with the PKCα, β1, β2, δ, ε and η isoforms in S2-013 cells. Immunoblotting of the immunoprecipitates revealed that ANX7 co-immunoprecipitated with PKC (Fig. 3A). PKC expression was not particularly high, but there were significant amounts in ANX7-immunoprecipitated complexes without PKC secretagogues. The effects of knocking down ANX7 on regulating PKC activity were investigated using Western blotting using an anti-phospho-PKC antibody (9379), which detects the classical PKCs (α, β1, β2 and γ) and novel PKCs (δ, ε, η and θ) when phosphorylated at a residue homologous to Thr514 of PKCγ (Fig. 3B). ANX7 knockdown induced phosphorylation of PKC in S2-013 cells, indicating that ANX7 plays a role in decreasing phosphorylated PKC. To investigate the subcellular colocalization of ANX7 and phosphorylated PKC, S2-013 cells were immunostained. ANX7 and phosphorylated PKC were colocalized in lamellipodial-like protrusions (arrows in Fig. 3C). Interestingly, ANX7 and phosphorylated PKC were recruited and colocalized to the leading edges during wound healing of S2-013 cells (arrows in Fig. 3D), indicating that phosphorylated PKC is associated with the anti-invasive function of ANX7. Since ANX7 could function in decreasing PKC activity (Fig. 3B), ANX7-dependent inhibition of cell invasion is likely to be associated with decreased activity of the specific classical or novel PKC isoforms. Thus, further experiments for analysis of the BART-ANX7-associated inhibition of cell invasion were focused on the classical and novel PKC isoforms to which the anti-phospho-PKC antibody (9379) reacted.

Phosphorylated PKC induces cell invasion of PDAC cells

A PKC stimulator, phorbol 12-myristate 13-acetate (PMA) is a potent tumor promoter [21] that induces migration of subconjunctival fibroblasts [19] and glioblastoma cells [9]. PMA interacts with and activates both classical and novel PKC isoforms [21]. Therefore, the effect of PMA on cell invasion of S2-013 and PANC-1 was investigated. Immunoblotting using anti-phospho-PKC antibody (9379) revealed that treatment with PMA increased active PKCs (Fig. 4A). PMA significantly stimulated cell invasion of S2-013 and PANC-1 in *in vitro* invasion assays (Fig. 4B), indicating that PMA-sensitive PKC isoforms contribute to the invasiveness of PDAC cells. To confirm that PMA-induced invasion was dependent on active PKCs, cells were initially treated with a PKC inhibitor (calphostin C, an inhibitor of both classical and novel PKCs) and then treated with PMA. Initial treatment with the PKC inhibitor prevented the PMA-induced increase in PKC activity (Fig. 4A) and inhibited PMA-mediated cell invasion of S2-013 and PANC-1 (Fig. 4B). These results indicate that specific isoforms of classical and novel PKCs could induce PDAC cell invasion.

Cell-cell adhesion can also influence motility [22]. Upon formation of cell-cell contacts, cells reduce their migration rate and cell-surface protrusion activity, and decrease their microtubule and actin-filament dynamics [23]. To determine the effect of the

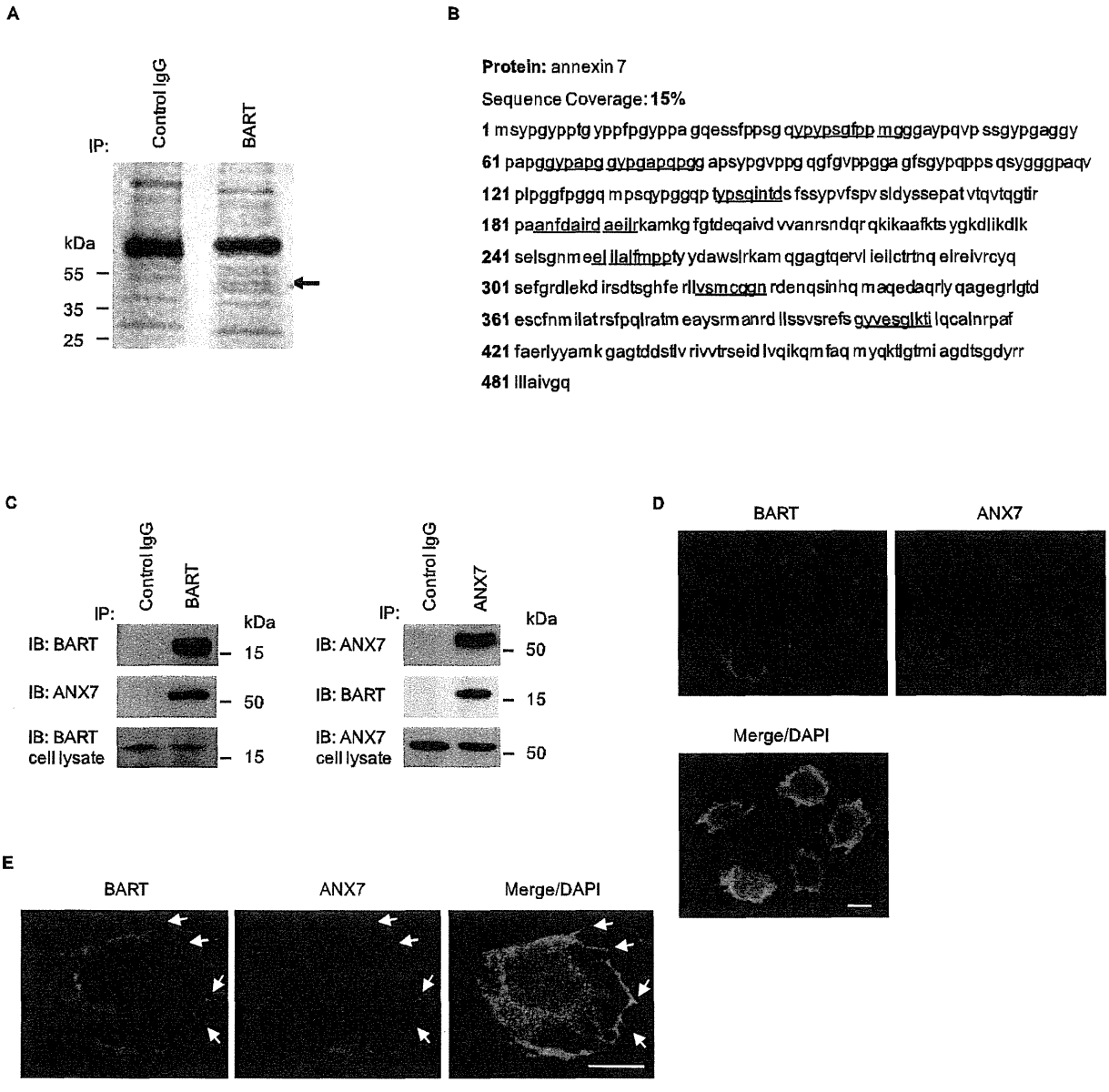

Figure 1. BART binds to ANX7 in lamellipodial-like protrusions. A. Immunoprecipitates from S2-013 cells using normal rabbit IgG (control) and anti-BART antibody were examined by silver stain analysis. Q-TOF-MS analysis investigated a prominent band in the BART immunoprecipitates (arrow). **B.** Percent coverage for ANX7 is represented by the identified peptides in the total protein sequence (accession number NM_004034). **C.** Immunoprecipitated endogenous BART or ANX7 from S2-013 were examined by Western blotting using anti-BART and anti-ANX7 antibodies. Normal rabbit or mouse IgG was used as an isotype control for BART and ANX7, respectively. **D.** Immunocytochemical staining of S2-013 cells using anti-BART (green) and anti-ANX7 (red) antibodies. Blue, DAPI staining. Bar, 10 μm. **E.** Arrows indicate that BART (green) and ANX7 (red) colocalize at lamellipodial-like protrusions of S2-013 cells. Blue, DAPI staining. Bar, 10 μm.
doi:10.1371/journal.pone.0035674.g001

classical and novel PKCs on cell-cell contact, S2-013 cells were incubated with PMA and immunofluorescence was performed using anti-E-cadherin and anti-β-catenin antibodies (Fig. 4C). PMA significantly reduced junction proteins at regions of cell-cell contact, indicating decreased peripheral localization of junction proteins, resulting in adherence junctions with decreased stability. These results suggest that PMA-sensitive PKCs play a role in decreasing stability of cell-cell contacts and, in turn, inducing cell invasion.

BART supports the binding of ANX7 to active PKC and functions in decreasing active PKC

To determine the effect of the BART-ANX7 complexes on regulating activity of PKC, the effects of BART knockdown on ANX7 affinity for constitutively activated PKCs by treatment with PMA were investigated (Fig. 5A). PMA stimulation caused significant increases in the amount of ANX7-PKC complexes in control cells, while there were no differences in BART RNAi S2-013 cells. Furthermore, whether binding could be inhibited by

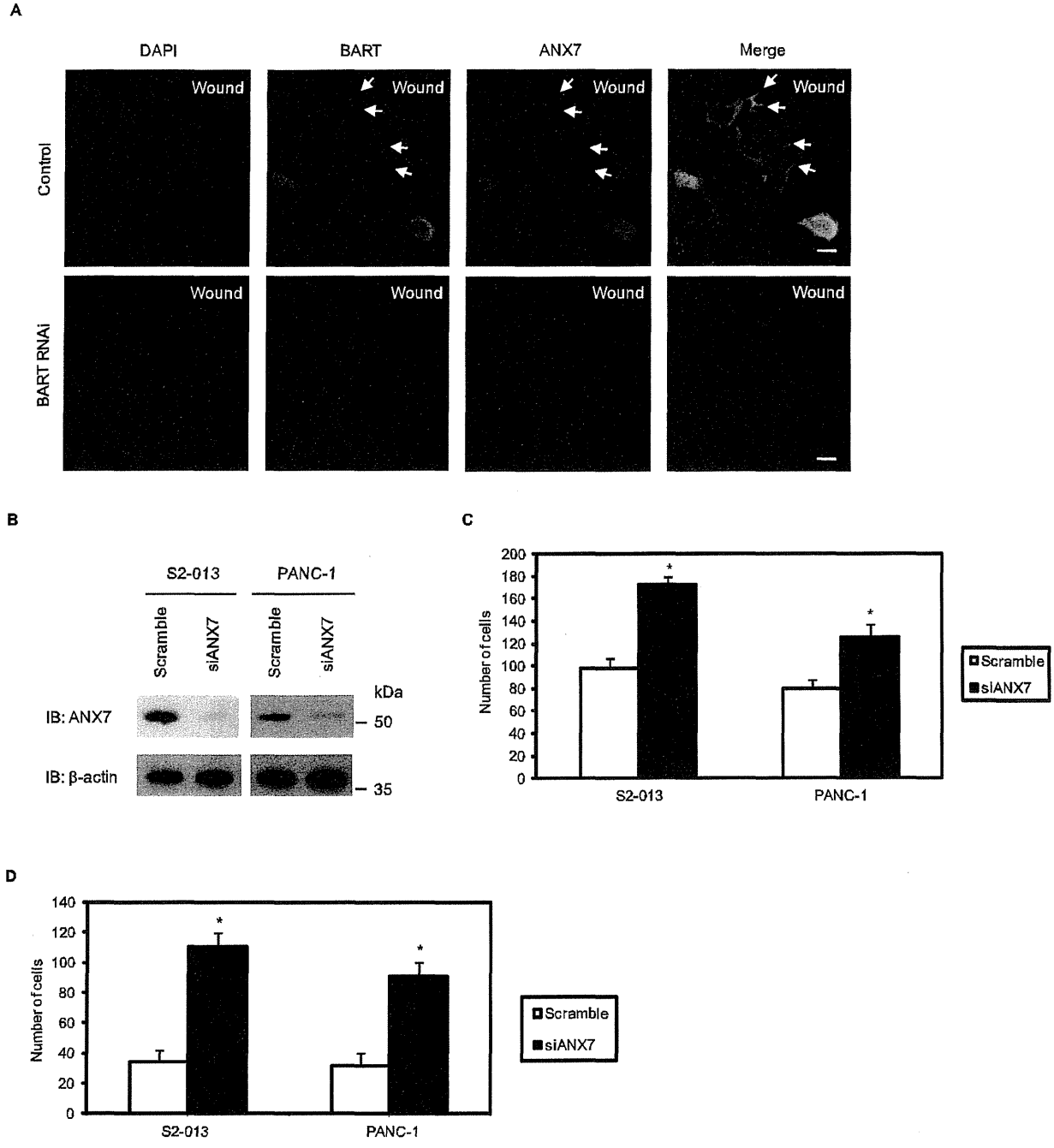

Figure 2. ANX7 suppresses cell motility and invasion in PDAC cells. A. Negative scrambled control (Scr-1) and BART RNAi (siBART-1) S2-013 cells in confluent cultures were wounded. After 4 h, the cells were immunostained using anti-BART (green) and anti-ANX7 (red) antibodies. Blue, DAPI staining. Arrows, colocalized BART and ANX7 at the leading edge of control cells. Bars, 10 μm. **B.** siRNA oligonucleotides targeting ANX7 (siANX7) and negative scrambled control were transiently transfected into S2-013 and PANC-1 cells. Western blotting validated ANX7 knockdown in both cell lines. **C.** Transwell motility assay of cells treated as in (B). Migrated cells in four fields per group were counted. Data are representative of three independent experiments. *Columns*, mean; *bars*, SD. *$p<0.005$ compared with control cells. **D.** Quantification of the two-chamber invasion assay of cells treated as in (B). Invaded cells in four fields per group were counted. Data are representative of three independent experiments. *Columns*, mean; *bars*, SD. *$p<0.001$ compared with control cells.
doi:10.1371/journal.pone.0035674.g002

PKC inhibitors prior to stimulation of control cells with PMA was assessed. Calphostin C and chelerythrine chloride (an inhibitor of PKCα, β, γ and δ) markedly decreased ANX7-PKC interaction in PMA-stimulated control cells (Fig. 5A). In addition, BART immunoprecipitated with increased amounts of ANX7 when S2-013 cells were treated with PMA, and preincubation with

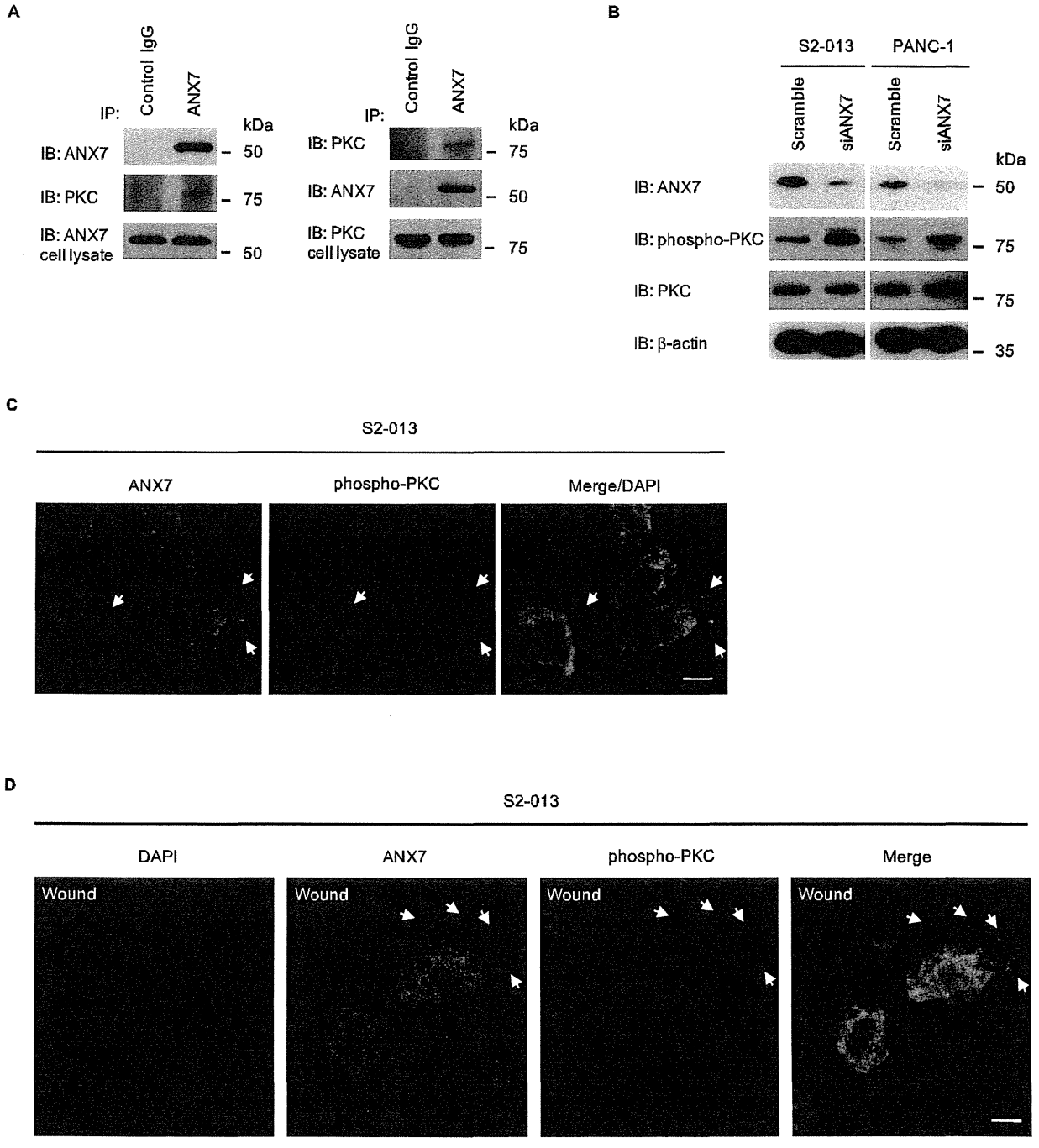

Figure 3. ANX7 and phosphorylated PKC are colocalized at the leading edges of migrating cells. A. Immunoprecipitation of endogenous ANX7 or PKC from S2-013 cells. Immunoprecipitates were examined by Western blotting using anti-ANX7 and anti-PKC antibodies. Normal mouse or rabbit IgG was used as the isotype control for ANX7 or PKC, respectively. **B.** Western blot with anti-PKC and anti-phospho-PKC antibodies showing S2-013 cells transiently transfected with siRNA for ANX7 as compared to cells transfected with scrambled control. **C.** Immunocytochemical staining in S2-013 cells, as determined with anti-ANX7 (green) and anti-phospho-PKC (red) antibodies. Blue, DAPI staining. Arrows, colocalized ANX7 and phosphorylated PKC at lamellipodial-like protrusions. Bar, 10 μm. **D.** Confluent S2-013 cells were wounded. After 4 h, the cells were immunostained using anti-ANX7 (green) and anti-phospho-PKC (red) antibodies. Blue, DAPI staining. Arrows, colocalized ANX7 and phosphorylated PKC at the leading edge. Bar, 10 μm.
doi:10.1371/journal.pone.0035674.g003

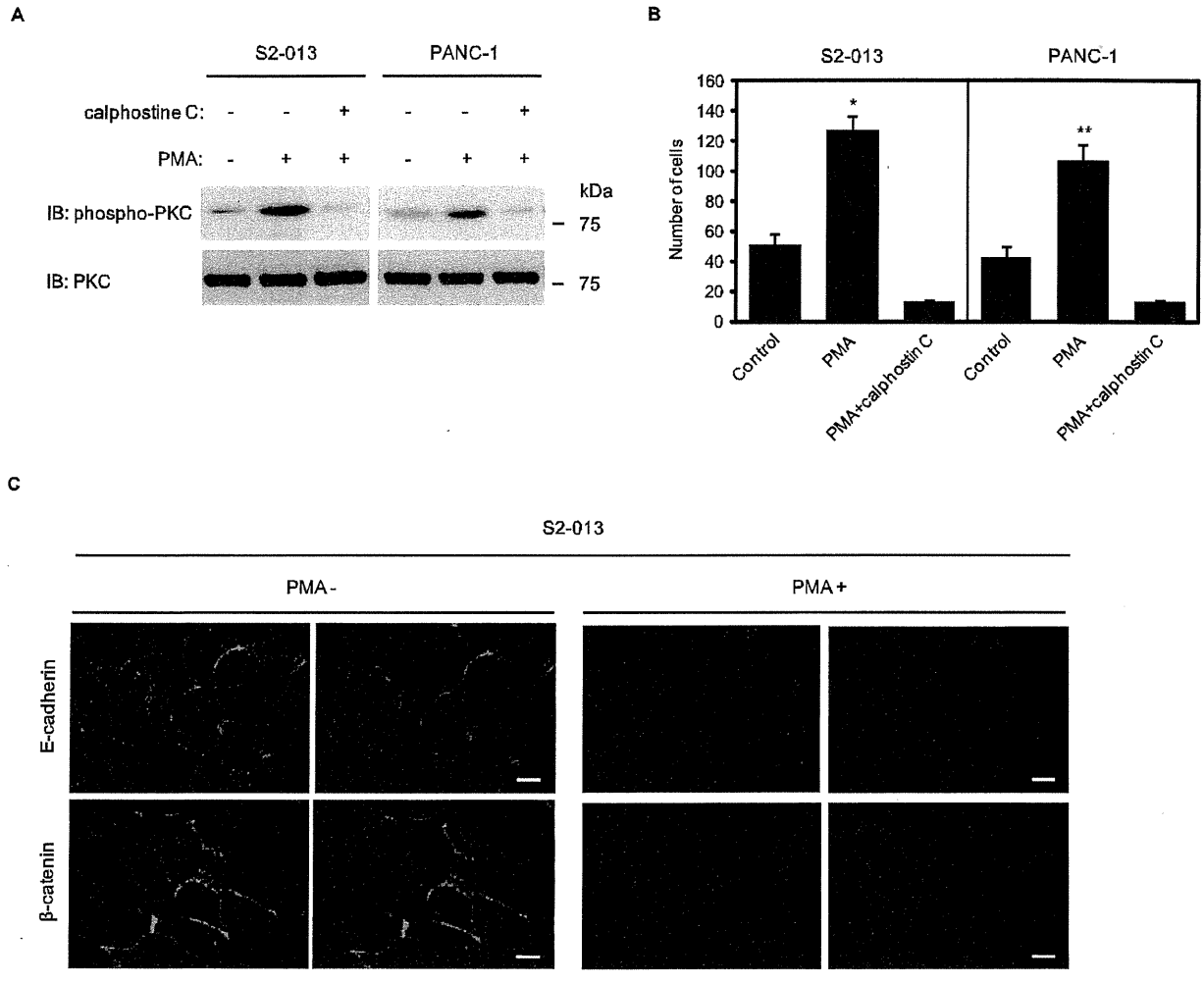

Figure 4. Effect of PMA on PDAC cell invasion. A. S2-013 and PANC-1 cells pretreated with or without calphostin C were treated with PMA, and PKC activity was assessed by Western blotting with an anti-phospho-PKC antibody. **B.** S2-013 and PANC-1 cells treated as in (A) were plated on Matrigel invasion chambers. Invaded cells in four fields per group were counted. Data are representative of three independent experiments. *Columns,* mean; *bars,* SD. *$p<0.001$; **$p<0.003$ as compared to non-treated control cells. **C.** S2-013 cells were treated with or without PMA, and immunocytochemical staining was performed using anti-E-cadherin and anti-β-catenin antibodies (green). Blue, DAPI staining; bars, 10 μm.
doi:10.1371/journal.pone.0035674.g004

calphostin C inhibited the increase in binding (Fig. 5B). Immunocytochemical analysis was performed to examine the intracellular localization of PMA-induced ANX7-PKC complexes in control and BART RNAi S2-013 cells (Fig. 5C). ANX7 colocalized with PMA-stimulated PKCs in control cells (arrows in Fig. 5C); however, BART knockdown prevented binding of ANX7 and PMA-stimulated PKCs (arrowheads in Fig. 5C). In addition, IP experiments using anti-phosphorylated PKC antibody (9379) confirmed that knocking down BART inhibited binding of ANX7 and phosphorylated PKC (Fig. 5D, E).

BART RNAi S2-013 cells had elevated active PKC levels and unchanged steady state levels of PKCs (Fig. 5F). This result indicates that BART may be associated with decreased levels of active PKC. We hypothesize that BART regulates interactions between ANX7 and active forms of target PKCs as a scaffold molecule and/or a cargo protein of ANX7, allows ANX7 to decrease target PKC activity, and in turn, inhibits cell invasion.

PKC activity is not directly regulated by ANX7

To investigate the role of PKC in regulating phosphorylation of ANX7, as previously reported in chromaffin cells [8], S2-013 and PANC-1 cells were metabolically labeled with [^{32}P]-orthophosphoric acid, and then stimulated with PMA. The radioactively labeled-ANX7 was immunoprecipitated with anti-ANX7 monoclonal antibody and was analyzed by phosphor imaging (Fig. 6A). If ANX7 is a substrate of specific PKCs, the level of ANX7 phosphorylation should result in significantly increased changes in response to PMA. However, PMA stimulation did not increase the levels of ANX7 phosphorylation in either cell line. Next, *in vitro* phosphorylation assays were used to determine whether PKC activity was directly regulated by ANX7 (Fig. 6B). Purified rat brain, with a purity of >95% and containing classical and novel PKC isoforms, was incubated with recombinant ANX7 protein with or without recombinant BART protein. ANX7 did not change the activity of PKCs and adding BART protein was not

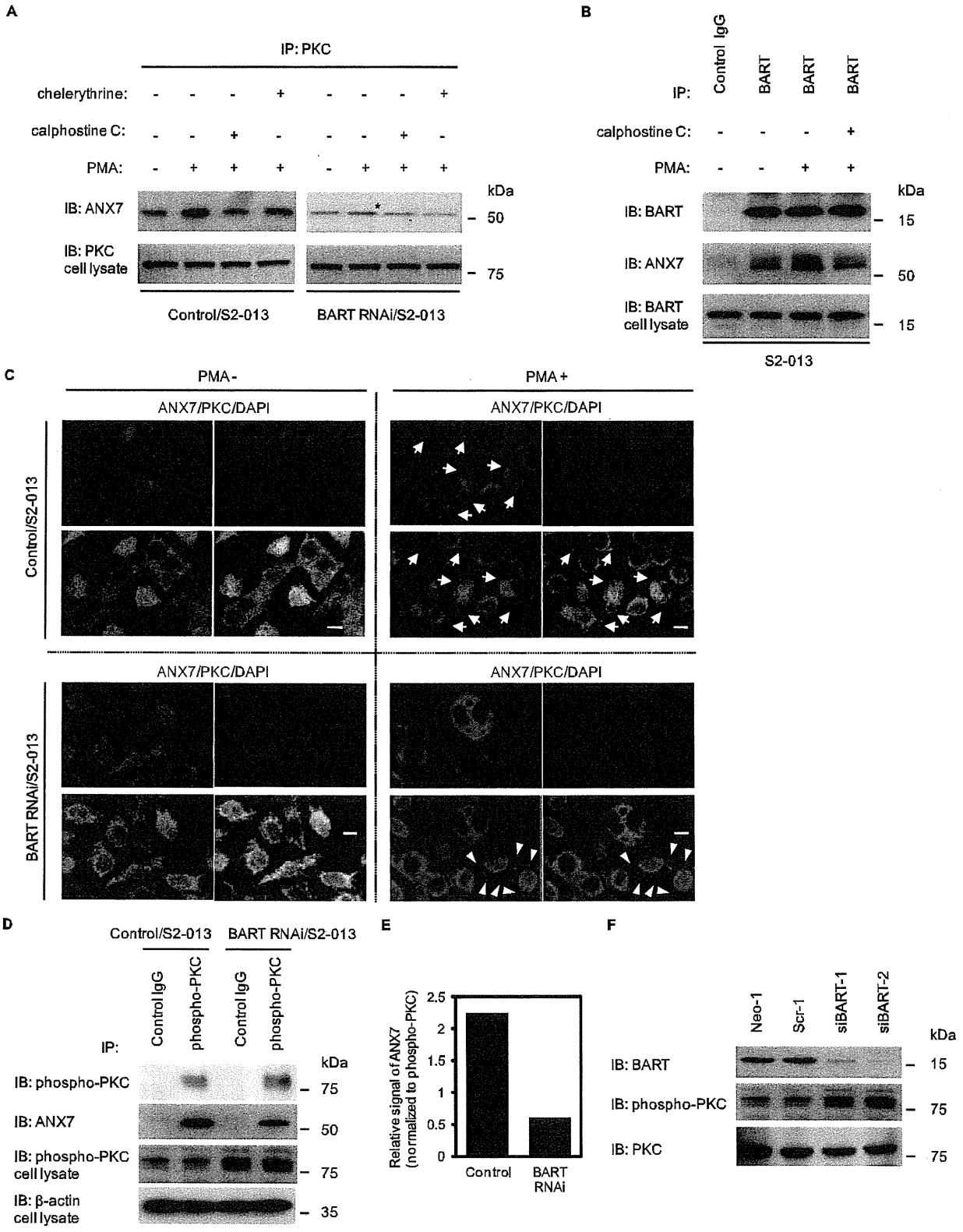

Figure 5. Effect of BART on regulating PKC activity through ANX7. A. Immunoprecipitation of PKC from control and BART RNAi S2-013 cells stimulated by PMA with or without pretreatment of calphostin C or chelerythrine chloride was examined by Western blotting using anti-ANX7 and anti-PKC antibodies. *, co-immunoprecipitated ANX7 with PKC in BART RNAi S2-013 cells. **B.** Immunoprecipitation of BART from S2-013 cells treated

as in (A) was examined by Western blotting using anti-ANX7 and anti-BART antibodies. **C.** Immunocytochemical staining of control (upper panels) and BART RNAi (lower panels) S2-013 cells stimulated by PMA using anti-PKC (green) and anti-ANX7 (red) antibodies. Blue, DAPI staining. Arrows, ANX7 colocalized with PMA-sensitive PKCs in control cells; arrowheads, PMA-sensitive PKCs not colocalized with ANX7 in BART RNAi cells. Bars, 10 μm. **D.** Immunoprecipitation of phosphorylated PKC from control and BART RNAi S2-013 cells was examined by Western blotting using anti-ANX7 and anti-phospho-PKC antibodies. **E.** Densitometric analysis of the results of Figure 5D. The level of ANX7 in the precipitates was assessed after normalizing ANX7 signals to phospho-PKC signals of cell lysates. **F.** Western blot with anti-BART and anti-phospho-PKC antibodies showing two S2-013 clones transfected with siRNA for BART (siBART-1 and 2) as compared to mock (Neo-1) and scrambled (Scr-1) control clones.
doi:10.1371/journal.pone.0035674.g005

associated with regulating PKC activity. These results suggest that ANX7 is not a substrate of PKC, and that ANX7 does not change phosphorylation levels of the target PKCs directly.

PKCα is associated with BART-ANX7 complexes

To identify specific isoforms of PKC that bind to ANX7 in this system, a precise expression profile of classical and novel PKCs was generated by Western blotting using individual anti-phospho-PKC antibodies in BART RNAi cells derived from S2-013 (Fig. 7A). Since phosphorylation levels of target PKCs were increased in BART RNAi cells (Fig. 5F), upregulated phospho-PKCs in BART RNAi cells were selected for further analysis. Among these, PKCα was significantly activated by BART knockdown in S2-013. In addition, PKCα was abundantly phosphorylated in ANX7 RNAi cells of S2-013 and PANC-1 (Fig. 7B). Next, binding of ANX7 with phosphorylated PKCα was demonstrated by immunoprecipitation and Western blotting analysis in S2-013 cells (Fig. 8A). Phospho-PKCη was not immunoprecipitated with ANX7. To investigate the subcellular colocalization of phosphorylated PKCα, S2-013 cells were immunostained. Phosphorylated PKCα was localized in lamellipodial-like protrusions (arrows in Fig. 8B). Additionally, ANX7 and phosphorylated PKCα were recruited to the leading edges during wound healing of control S2-013 cells (upper panels in Fig. 8C). Depletion of BART did not induce accumulation of ANX7 at the leading edges and subsequent colocalization with phosphorylated PKCα (lower panels in Fig. 8C). These results indicate that PKCα is interdependently associated with BART and ANX7 in modulating PDAC cell migration.

Specific inhibitors of PKCα inhibit increased cell migration by knockdown of BART and ANX7

To examine whether PKCα signaling is involved in increased migration by BART or ANX7 knockdown in S2-013, a PKCα/β1 inhibitor Ro-32-0432 and a specific PKCα inhibitor safingol were applied in *in vitro* invasion assays. As shown in Fig. 9A and 9B, phosphorylated PKCα was specifically decreased by Ro-32-0432 and safingol treatment, but expressions of phospho-PKCη was not changed. The greatest migration of S2-013 cells occurred after knocking down BART or ANX7; however, the increased migration was inhibited by preincubation with Ro-32-0432 (Fig. 9C) and safingol (Fig. 9D). Increased invasiveness by BART or ANX7 knockdown was not prevented by preincubation with a myristoylated pseudosubstrate PKCη inhibitor (Fig. 9E) and a PKCδ inhibitor (rottlerin; data not shown). These results suggest that activation of PKCα is required for PDAC cell migration induced by BART or ANX7 knockdown.

Discussion

PDAC is one of the deadliest cancers due to its ability to extensively invade surrounding tissues and metastasize at an early stage [24]. Extensive local infiltration and metastasis are the main causes of death in PDAC [25]. In light of the role of BART in inhibiting PDAC cell invasion, this study was designed to identify the BART binding proteins associated with PDAC cell invasiveness. The salient features of this report are as follows:

(i) BART and ANX7 may function together in complex to inhibit cell migration.

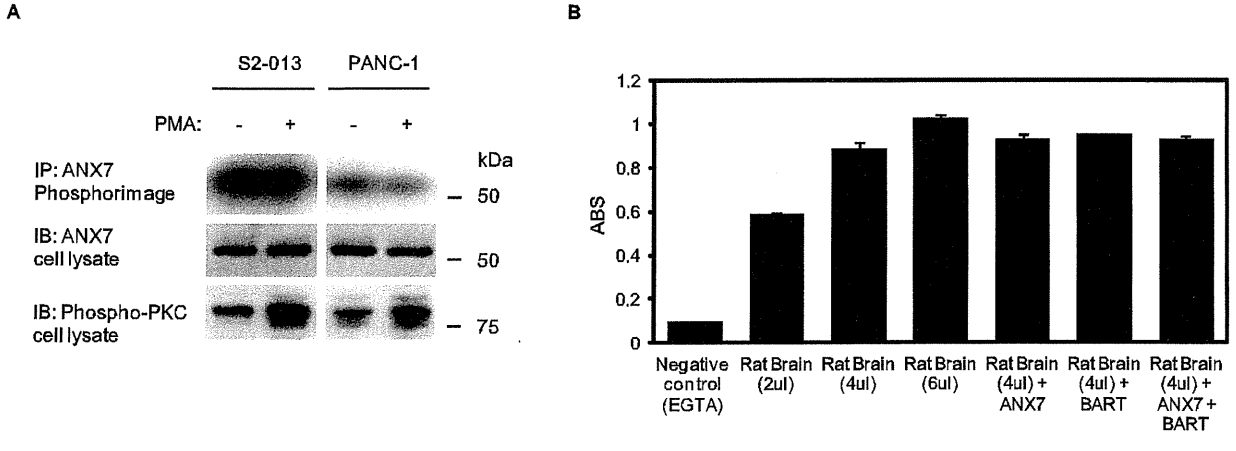

Figure 6. PKC phosphorylation is not directly regulated by ANX7. A. S2-013 and PANC-1 cells were prelabeled with [^{32}P]-orthophosphoric acid and stimulated or not with PMA. ANX7 was immunoprecipitated, separated by SDS-PAGE, and analyzed by autoradiography. An immunoblot was performed on the cell lysate as a loading control. **B.** *In vitro* phosphorylation assays to investigate the effect of BART and ANX7 on PKC-phosphorylation. Purified rat brain was incubated with recombinant ANX7 with or without recombinant BART. The reaction products were analyzed by an ELISA assay. ABS on *Y*-axis means absorbance at 492 nm as reference measured with a microplate reader.
doi:10.1371/journal.pone.0035674.g006

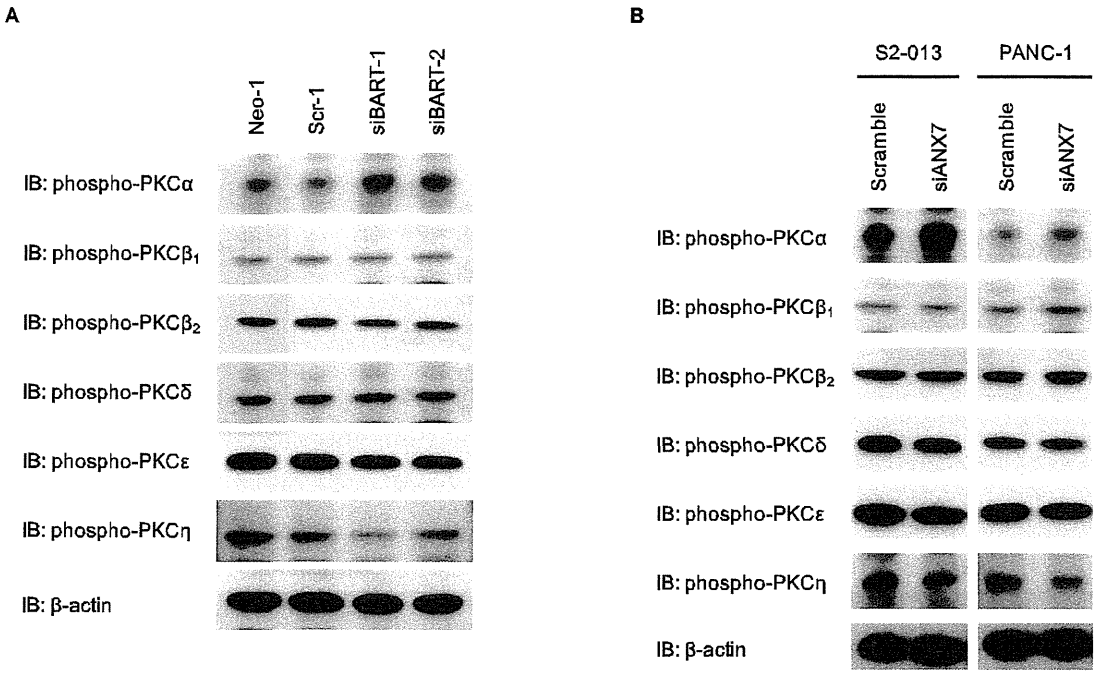

Figure 7. The activity of PKCα is increased by suppression of BART and ANX7. A. Western blot with antibodies against the classical and novel PKC isoforms showing two S2-013 clones transfected with siRNA for BART as compared to mock and scrambled control clones. **B.** siRNA oligonucleotides targeting ANX7 and negative scrambled control were transiently transfected into S2-013 and PANC-1 cells. Western blot with antibodies against the classical and novel PKC isoforms was performed.
doi:10.1371/journal.pone.0035674.g007

(ii) BART and ANX7 may inhibit cell invasion by decreasing active PKC at leading edges.

(iii) Phosphorylated PKCα is responsible for the increased invasiveness of PDAC cells seen with BART or ANX7 knockdown. PKCα is interdependently associated with BART and ANX7 in modulating invasiveness of PDAC cells.

Frequent loss of ANX7 expression was observed in prostate cancer, especially in metastasis and local recurrence of hormone refractory disease [7]. Whereas null *ANX7−/−* mice die during embryogenesis, ANX7 heterozygous mice (*ANX7+/−*) develop, mature, and age normally, and more interestingly, have a cancer-prone phenotype [10]. A broad range of spontaneous tumors have been detected in *ANX7+/−* mice, including in liver, prostate, endometrium, salivary gland, and thymus [11]. In the mouse, haploinsufficiency of ANX7 expression appears to drive progression to cancer because of genomic instability through a discrete signaling pathway involving other tumor suppressor genes, DNA-repair genes, and apoptosis-related genes. Our data suggest that BART and ANX7 play a role in decreasing the phosphorylation level of PKCα in PDAC cells. *In vitro* experiments failed to demonstrate that ANX7 directly decreased activity of PKC (Fig. 6B); however, Fig. 6A shows definitively that ANX7 was not a substrate for PKC in PDAC cells. Although the mechanism by which ANX7 regulates PKC activity remains unknown, it is notable that BART and ANX7 could function together to decrease the activity of the PKCα isoform and, in turn, suppress invasiveness of PDAC cells. This study enabled evaluation of a cellular signaling pathway regulated by the *ANX7* tumor suppressor gene in PDAC. Further studies are needed to determine which molecules directly suppress PKCα, and to identify precise substrates of PKCα, in order to understand the mechanisms involved in BART-ANX7-mediated inhibition of cell invasion.

The role of PKCα in PDAC cell migration has not been extensively studied. Several lines of evidence indicate that PKCα plays critical roles in cell proliferation/migration/invasion, including human poorly differentiated hepatic cancer [26], endometrial cancer [27] and gastric cancer [28]. Cell signaling pathways involving the PKC family are initiated by binding of a ligand, such as a growth factor, to its respective cell surface receptor, which triggers the breakdown of phospholipids by phospholipases C and D and production of diacylglycerol (DAG). DAG binds to and activates most PKC isoforms, which then translocate to specific subcellular compartments that vary depending on the PKC isoform and cell type. Ultimately, MAPKs, including the extracellular-signal-regulated protein kinase (ERK), c-jun N-terminal kinase (JNK), and p38MAPK, play a crucial role in cell migration mediated by PMA-activated PKCs [19,29]. That BART and ANX7 abrogate phosphorylation of ERK in PDAC cells has been demonstrated (data not shown), suggesting that PKCα may be associated with modulating the ERK activity possibly associated with BART-ANX7-related inhibition of invasiveness. Furthermore, it is possible that PKCα-induced exocytosis modulates cell migration. Thus, future studies of PKCα are warranted to further characterize its exocitic function and elucidate its potential contribution to cell migration.

In summary, the findings presented in this study are supportive of the pivotal roles of BART in the coordinated regulation of PKCα activity *via* binding with ANX7. The functional significance of the association of BART, ANX7 and PKCα in modulating invasiveness of PDAC cells was established. It is possible that BART and ANX7 can distinctly regulate the downstream

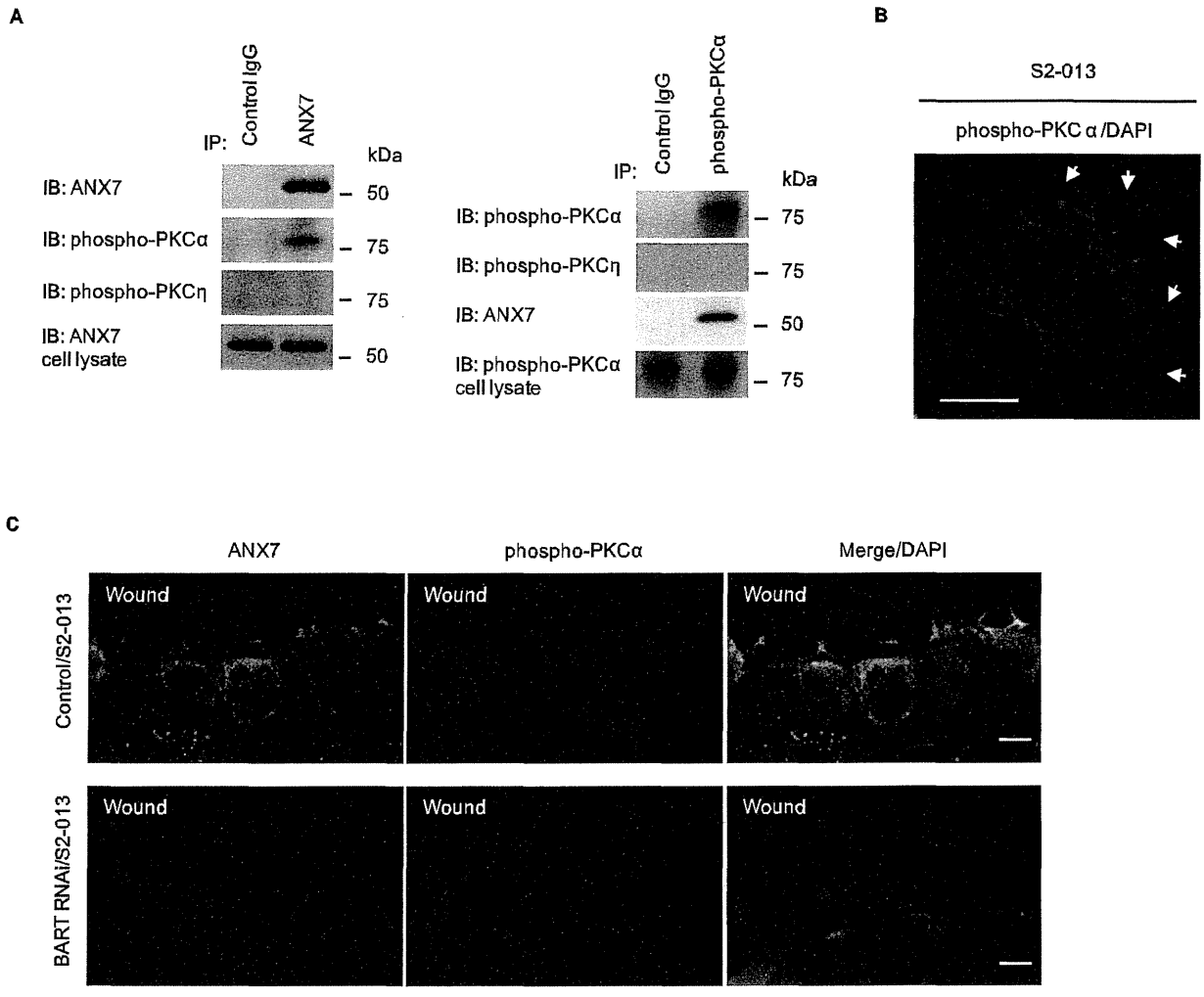

Figure 8. BART supports the colocalization of ANX7 and phospho-PKCα at the leading edges of migrating cells. A. Immunoprecipitation of ANX7 (left panels) or phospho-PKCα (right panels) from S2-013 cells was examined by Western blotting using antibodies against ANX7, phospho-PKCα and phospho-PKCη. **B.** Immunocytochemical staining in S2-013 cells, as determined with anti-phospho-PKC antibody (green). Blue, DAPI staining. Arrows, phosphorylated PKC at lamellipodial-like protrusions. Bar, 10 μm. **C.** Confluent cultures of control and BART RNAi S2-013 cells were wounded. After 4 h, the cells were immunostained using anti-ANX7 (green) and anti-phospho-PKCα (red) antibodies. Blue, DAPI staining. Bars, 10 μm.
doi:10.1371/journal.pone.0035674.g008

signaling of PKCα that is potentially relevant to cell invasion by acting as anti-invasive molecules. Further studies to investigate precise mechanisms of action are warranted.

Materials and Methods

Reagents and antibodies

PMA and PKC inhibitors (calphostin C, chelerythrine chloride, Ro-32-0432, safingol, rottlerin and a myristoylated pseudosubstrate PKCη inhibitor) were purchased from Calbiochem (San Diego, CA). PMA and the PKC inhibitors were prepared as 10 mM stock solutions in dimethyl sulfoxide or distilled water.

Rabbit anti-BART antibody (10090-2-AP) was purchased from ProteinTech (Chicago, IL). Monoclonal antibodies against ANX7 (610669), Rac1 (610650) and β-catenin (610154) were obtained from BD Transduction Laboratory (Palo Alto, CA). Polyclonal antibodies against pan-PKC (sc-10800), PKCα (sc-208), PKCβ1 (sc-209), PKCβ2 (sc-210), PKCδ (sc-213), PKCε (sc-214) and PKCη (sc-215) were obtained from Santa Cruz Biotechnology (Santa Cruz, CA). The rabbit anti-phospho-pan-PKC antibody (9379) was purchased from Cell Signaling (Grand Island, NY), and an anti-phospho-PKCα antibody (ab23513) was obtained from Abcam (Cambridge, MA). Polyclonal antibodies against phospho-PKCβ1 (sc-101776), -PKCδ (sc-101777), and -PKCε (sc-12355) were purchased from Santa Cruz Biotechnology, and polyclonal antibodies against phospho-PKCβ2 (07-873) and -PKCη (07-877) were obtained from Millipore (Billerica, MA).

Cell culture

The human PDAC cell line S2-013, a subline of SUIT-2, was obtained from Dr. T. Iwamura [20]. The human PDAC cell line PANC-1 was obtained from ATCC. Cells were grown in Dulbecco's modified Eagle's medium (DMEM; Gibco-BRL,

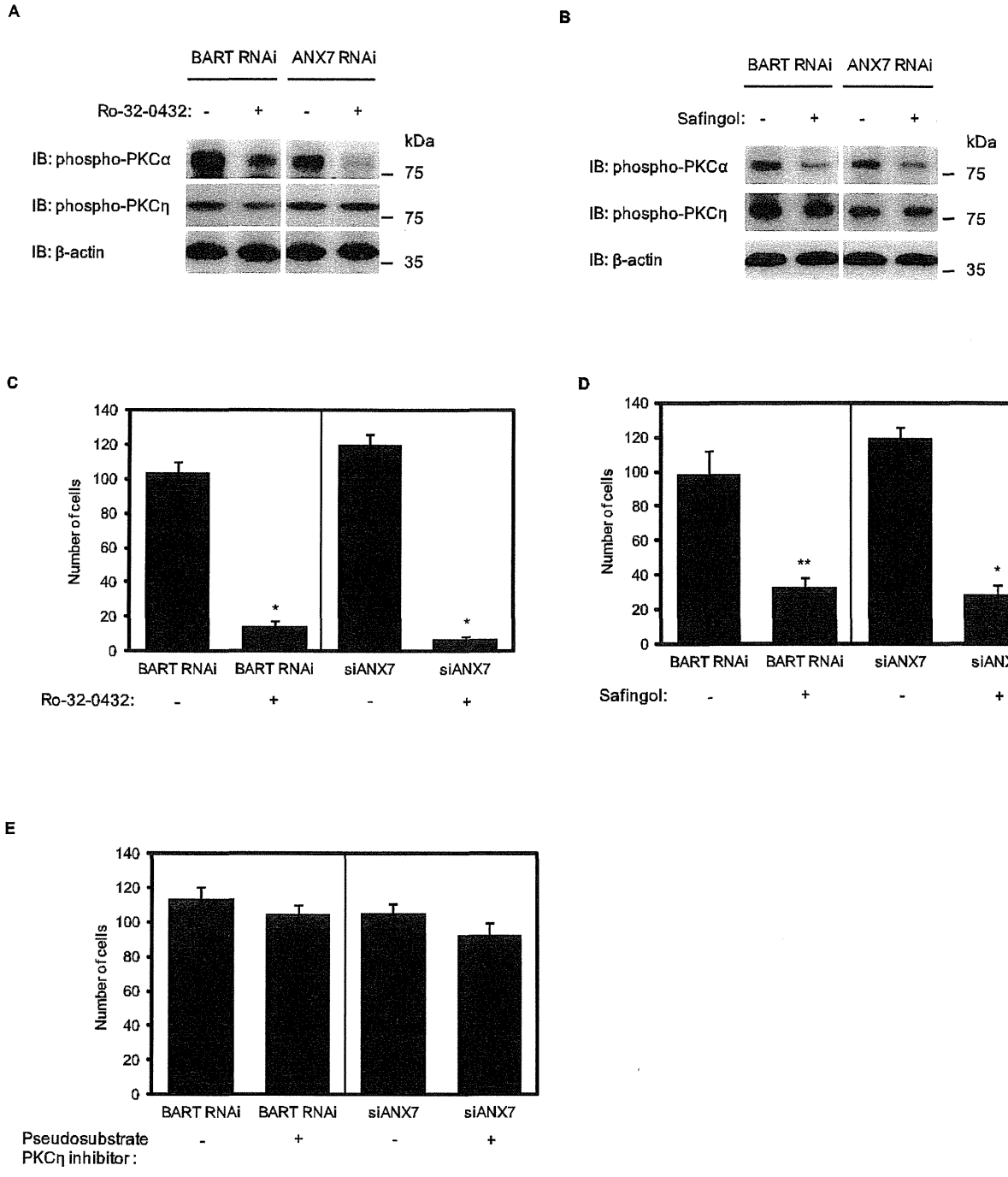

Figure 9. PKCα is associated with increased cell invasion by knockdown of BART and ANX7. A. BART RNAi S2-013 cells and S2-013 cells transiently transfected with ANX7-siRNA were pretreated with or without Ro-32-0432. The activity of PKCα and η was assessed by Western blotting. **B.** Cells shown in (A) were pretreated with or without safingol. The activity of PKCα and PKCη was assessed by Western blotting. **C.** The effect of Ro-32-0432 on cell invasion was investigated using the transwell invasion assay. Migrated cells in four fields per group were counted. Data are representative of three independent experiments. *Columns*, mean; *bars*, SD. *$p<0.001$ compared with non-treated cells. **D.** The effect of safingol on cell invasion was investigated using the transwell invasion assay. Data are representative of three independent experiments. *Columns*, mean; *bars*, SD. *$p<0.001$; **$p<0.003$ compared with non-treated cells. **E.** The effect of rottlerin and pseudosubstrate PKCη inhibitor on cell invasion was investigated using the transwell invasion assay. Data are representative of three independent experiments. *Columns*, mean; *bars*, SD.
doi:10.1371/journal.pone.0035674.g009

Carlsbad, CA) supplemented with 10% heat-inactivated fetal calf serum (FCS) at 37°C in a 5% CO_2, humid atmosphere.

Immunoprecipitation and mass spectrometric analysis of BART

S2-013 cells were lysed in lysis buffer [20 mM HEPES (pH 7.4), 100 mM KCl, 5 mM $MgCl_2$, 0.5% Triton X-100, and protease inhibitor cocktail tablets (Roche, Penzberg, Germany)]. Equal amounts of S2-013 cell lysates were incubated with 2 μg of anti-BART antibody or normal rabbit IgG (isotype control) and protein G Sepharose. Co-immunoprecipitated proteins were separated on a 4% to 20% gradient SDS-PAGE and then silver stained. Bands precipitated by the anti-BART antibody were excised, digested with trypsin and analyzed using a Q-TOF Ultima tandem mass spectrometer (Waters, Milford, MA) with electrospray ionization. Database searches of the acquired MS/MS spectra were performed using MASCOT v1.9.0 (Matrix Science, Boston, MA).

In vivo binding of BART with ANX7

S2-013 cells were lysed with lysis buffer and immunoprecipitated with 2 μg of anti-BART or anti-ANX7 antibody. To examine the interaction of endogenous BART with ANX7, immune complexes were analyzed by Western blotting with anti-BART and anti-ANX7 antibodies.

Confocal immunofluorescence microscopy

Cells were fixed with 4% paraformaldehyde, permeabilized with 0.1% Triton X-100, covered with blocking solution (3% BSA/PBS), and then incubated with the primary antibody for 1 h. Alexa 488 and Alexa 594-conjugated secondary antibodies (Molecular Probes, Carlsbad, CA) were used. Each specimen was visualized using a Zeiss LSM 510 META microscope (Carl Zeiss, Gottingen, Germany).

siRNA-expressing constructs and the generation of stable cell lines

The methods used were as previously reported [4]. We used a pSUPERgfp vector (OligoEngine, Seattle, WA) for expression of siRNA. The target sequences for the scrambled negative control and for BART were 5′-TTCTCCGAACGTGTCACGT-3′ and 5′-CATGGCAGCCTTCACCACA-3′, respectively. S2-013 and PANC-1 cells were transfected with either empty Neo-pSUPERgfp, a scrambled oligo-pSUPERgfp negative control, or a plasmid designed to express siRNA to BART, using FuGENE6 (Roche), according to the manufacturer's instructions. Cells were selected in medium containing 500 μg/mL of geneticin to generate stable pSUPERgfp cell lines. Western blotting was performed to analyze the protein levels of the single clones.

siRNA treatment

RNAi targeting ANX7 and scrambled negative control siRNA oligonucleotides were purchased from Santa Cruz Biotechnology (29690 and 37007). For assays to examine the effect of siRNAs on ANX7 expression, S2-013 and PANC-1 cells that express ANX7 were plated in six-well plates. After 20 h, the cells were transfected with 80 pmols of siRNA in siRNA transfection reagent (Santa Cruz), following the manufacturer's instructions.

Transwell motility assay

Cells (3.0×10^4) were plated in the upper chamber of BD BioCoat Control Culture Inserts (24-well plates, 8 μm pore size; Becton Dickinson, San Jose, CA). Serum-free culture medium was added to the upper chamber, and medium containing 5% FCS was added to the lower chamber. Cells were incubated on the membranes for 12 h, and motility was quantified.

Matrigel invasion assay

The two-chamber invasion assay was used to assess cell invasion (24-well plates, 8 μm pore size, membrane coated with a layer of Matrigel extracellular matrix proteins; Becton Dickinson). Cells (4.0×10^4) were seeded in serum-free medium into the upper chamber and allowed to invade toward 5% FCS (the chemoattractant) in the lower chamber. After 20 h incubation, the number of invading cells at the bottom of the membrane was estimated under microscopic observation by counting three independent visual fields.

BART or ANX7 RNAi S2-013 cells were preincubated for 30 min in serum-free medium containing 250 nM Ro-32-0432, 10 mM safingol, 5.0 μM rottlerin, or 5.0 μM myristoylated PKCη pseudosubstrate inhibitor. These preincubated cells were used in the two-chamber invasion assay to assess cell invasion.

Wound healing immunostaining assay

A wound in the form of a cross was made through a confluent cell monolayer with a plastic pipette tip and cells were then allowed to polarize and migrate toward the wound. After 4 h, cells were immunostained with primary antibody and then incubated with fluorophore-conjugated secondary antibodies as described above. Each specimen was visualized with a Zeiss LSM 510 META microscope.

Stimulation of PKC by PMA and inhibition of kinase activity by specific inhibitors

Cells were incubated in FCS-free medium for 24 h. 1 h prior to incubation with PMA, cells were preincubated at 37°C in Ca^{2+}-free buffer A [25 mM Hepes (pH 7.2), 118 mM NaCl, 4.2 mM KCl, 1.2 mM $MgCl_2$, 10 mM $NaHCO_3$, 10 mM glucose, 0.1% bovine serum albumin] containing 50 nM calphostin C or 1.0 μM chelerythrine chloride, both specific PKC inhibitors. Next, cells were cultured for 30 min at 37°C in the presence of 100 nM PMA in buffer B (buffer A with 2.2 mM $CaCl_2$ added). These cells were subjected to further analysis.

[^{32}P]-orthophosphoric acid labeling and treatment of PDAC cells with PMA and PKC inhibitors

Cells (2×10^6/dish, 60 mm) were labeled with [^{32}P]-orthophosphoric acid (1.0 mCi/ml) in phosphate-free Eagle's minimal essential medium containing 10% dialyzed FCS for 3 h at 37°C. The cells were washed once with buffer A. The cells were pretreated for 1 h at 37°C with or without the PKC inhibitors 50 nM calphostin C or 1.0 μM chelerythrine chloride in buffer A and were then stimulated to secrete by incubation for 30 min at 37°C in the presence (or absence) of 100 nM PMA in buffer B.

Recombinant ANX7

The entire coding sequence of ANX7 cDNA was amplified by RT-PCR. The product was subsequently inserted into the pIEx-7 Ek/LIC vector (Novagen, Madison, WI) to produce a fusion protein, bearing an N-terminal 6-histidine tag. Sf9 cells (Novagen) were transiently transfected using the Insect GeneJuice Transfection Reagent (Novagen), according to the manufacturer's instructions. Transfected cells were lysed in CytoBuster Protein Extraction Reagent (Novagen) and centrifuged at 15,000× g for 15 min. The supernatant was combined with the Ni-NTA His-Bind Resin (Novagen), and bound proteins were eluted. Western

blotting using an anti-ANX7 antibody was performed to identify the fractions containing ANX7. The fractions, corresponding to apparently pure proteins, were pooled, and dialyzed against storage buffer that consisted of 20 mM HEPES (pH 7.4), 20 mM KCl, and 10% glycerol. The samples were stored at −80°C.

In vitro detection of PKC phosphorylation

A 0.05 unit (0.035 μg) of purified rat brain, with a purity of >95% and containing classical and novel PKC isoforms (Calbiochem) was incubated at 30°C for 20 min with 0.5 μmol of recombinant ANX7 with or without 0.3 μmol recombinant BART in a final volume of 30 μl of reaction buffer [25 mM Tris-HCl (pH 7.0), 5 mM β-mercaptoethanol, 3 mM $MgCl_2$, 2 mM $CaCl_2$, 1 mM EGTA, 0.5 mM EDTA, 0.1 mM ATP, 50 μg/ml phosphatidylserine]. To determine PKC phosphorylation, the reaction products were analyzed by an ELISA assay using PKLight Protein Kinase Assay kits (Lonza, Basel, Switzerland) according to the manufacturer's instructions.

Statistical analysis

The significance of differences between groups was determined using the Student's *t*-test, the Mann-Whitney *U* test, or Fisher's exact test, as appropriate. Differences having *P* values <0.05 were considered statistically significant.

Acknowledgments

We thank Michael Hollingsworth for many helpful experimental suggestions. We also thank Aki Tanouchi for her excellent technical assistance.

Author Contributions

Conceived and designed the experiments: KT. Performed the experiments: KT. Analyzed the data: KT TS. Contributed reagents/materials/analysis tools: KT TS. Wrote the paper: KT. Edited the manuscript: KY TS.

References

1. Sharer JD, Kahn RA (1999) The ARF-like 2 (ARL2)-binding protein, BART. Purification, cloning, and initial characterization. J Biol Chem 274: 27553–27561.
2. Clark J, Moore L, Krasinskas A, Way J, Battey J, et al. (1993) Selective amplification of additional members of the ADP-ribosylation factor (ARF) family: cloning of additional human and Drosophila ARF-like genes. Proc Natl Acad Sci U S A 90: 8952–8956.
3. Zhou C, Cunningham L, Marcus AI, Li Y, Kahn RA (2006) Arl2 and Arl3 regulate different microtubule-dependent processes. Mol Biol Cell 17: 2476–2487.
4. Taniuchi K, Nishimori I, Hollingsworth MA (2011) Intracellular CD24 inhibits cell invasion by post-transcriptional regulation of BART through interaction with G3BP. Cancer Res 71: 895–905.
5. Taniuchi K, Nishimori I, Hollingsworth MA (2011) The N-terminal domain of G3BP enhances cell motility and Invasion by posttranscriptional regulation of BART. Mol Cancer Res 9: 856–866.
6. Taniuchi K, Iwasaki S, Saibara T (2011) BART inhibits pancreatic cancer cell invasion by inhibiting ARL2-mediated RhoA inactivation. Int J Oncol 39: 1243–1252.
7. Srivastava M, Atwater I, Glasman M, Leighton X, Goping G, et al. (1999) Defects in inositol 1,4,5-trisphosphate receptor expression, Ca(2+) signaling, and insulin secretion in the anx7(+/−) knockout mouse. Proc Natl Acad Sci U S A 96: 13783–13788.
8. Caohuy H, Pollard HB (2001) Activation of annexin 7 by protein kinase C in vitro and in vivo. J Biol Chem 276: 12813–12821.
9. Park MJ, Park IC, Hur JH, Rhee CH, Choe TB, et al. (2000) Protein kinase C activation by phorbol ester increases in vitro invasion through regulation of matrix metalloproteinases/tissue inhibitors of metalloproteinases system in D54 human glioblastoma cells. Neurosci Lett 290: 201–204.
10. Srivastava M, Bubendorf L, Srikantan V, Fossom L, Nolan L, et al. (2001) ANX7, a candidate tumor suppressor gene for prostate cancer. Proc Natl Acad Sci U S A 98: 4575–4580.
11. Srivastava M, Montagna C, Leighton X, Glasman M, Naga S, et al. (2003) Haploinsufficiency of Anx7 tumor suppressor gene and consequent genomic instability promotes tumorigenesis in the Anx7(+/−) mouse. Proc Natl Acad Sci U S A 100: 14287–14292.
12. Mellor H, Parker PJ (1998) The extended protein kinase C superfamily. Biochem J 332: 281–92.
13. Musashi M, Ota S, Shiroshita N (2000) The role of protein kinase C isoforms in cell proliferation and apoptosis. Int J Hematol 72: 12–19.
14. Nishizuka Y (1995) Protein kinase C and lipid signaling for sustained cellular responses. FASEB J 9: 484–496.
15. Nishizuka Y (1988) The molecular heterogeneity of protein kinase C and its implications for cellular regulation. Nature 334: 661–665.
16. Edwards AS, Newton AC (1997) Phosphorylation at conserved carboxyl-terminal hydrophobic motif regulates the catalytic and regulatory domains of protein kinase C. J Biol Chem 272: 18382–18390.
17. Schonwasser DC, Marais RM, Marshall CJ, Parker PJ (1998) Activation of the mitogen-activated protein kinase/extracellular signal-regulated kinase pathway by conventional, novel, and atypical protein kinase C isotypes. Mol Cell Biol 18: 790–798.
18. Mauro LV, Grossoni VC, Urtreger AJ, Yang C, Colombo LL, et al. (2010) PKC Delta (PKCdelta) promotes tumoral progression of human ductal pancreatic cancer. Pancreas 39: e31–41.
19. Nomura N, Nomura M, Takahira M, Sugiyama K (2007) Phorbol 12-myristate 13-acetate-activated protein kinase C increased migratory activity of subconjunctival fibroblasts via stress-activated protein kinase pathways. Mol Vis 13: 2320–2327.
20. Iwamura T, Katsuki T, Ide K (1987) Establishment and characterization of a human pancreatic cancer cell line (SUIT-2) producing carcinoembryonic antigen and carbohydrate antigen 19-9. Jpn J Cancer Res 78: 54–62.
21. Ron D, Kazanietz MG (1999) New insights into the regulation of protein kinase C and novel phorbol ester receptors. FASEB J 13: 1658–1676.
22. Huttenlocher A, Lakonishok M, Kinder M, Wu S, Truong T, et al. (1998) Integrin and cadherin synergy regulates contact inhibition of migration and motile activity. J Cell Biol 141: 515–526.
23. Waterman-Storer CM, Salmon WC, Salmon ED (2000) Feedback interactions between cell-cell adherens junctions and cytoskeletal dynamics in newt lung epithelial cells. Mol Biol Cell 11: 2471–2483.
24. Baumgart M, Heinmöller E, Horstmann O, Becker H, Ghadimi BM (2005) The genetic basis of sporadic pancreatic cancer. Cell Oncol 27: 3–13.
25. Ahrendt SA, Pitt HA (2002) Surgical management of pancreatic cancer. Oncology 16: 725–734.
26. Wu TT, Hsieh YH, Hsieh YS, Liu JY (2008) Reduction of PKC alpha decreases cell proliferation, migration, and invasion of human malignant hepatocellular carcinoma. J Cell Biochem 103: 9–20.
27. Haughian JM, Bradford AP (2009) Protein kinase C alpha (PKCalpha) regulates growth and invasion of endometrial cancer cells. J Cell Physiol 220: 112–118.
28. Jiang XH, Tu SP, Cui JT, Lin MC, Xia HH, et al. (2004) Antisense targeting protein kinase C alpha and beta1 inhibits gastric carcinogenesis. Cancer Res 64: 5787–5794.
29. Huang C, Jacobson K, Schaller MD (2004) MAP kinases and cell migration. J Cell Sci 117: 4619–4628.